



ARCHIVIO ISTITUZIONALE DELLA RICERCA

Alma Mater Studiorum Università di Bologna Archivio istituzionale della ricerca

Epigenetic signatures of stress adaptation and flowering regulation in response to extended drought and recovery in *Zea mays*

This is the final peer-reviewed author's accepted manuscript (postprint) of the following publication:

Published Version:

Epigenetic signatures of stress adaptation and flowering regulation in response to extended drought and recovery in *Zea mays* / Forestan C.; Farinati S.; Zambelli F.; Pavesi G.; Rossi V.; Varotto S.. - In: PLANT, CELL AND ENVIRONMENT. - ISSN 0140-7791. - ELETTRONICO. - 43:1(2020), pp. 55-75. [10.1111/pce.13660]

This version is available at: <https://hdl.handle.net/11585/868498> since: 2022-02-24

Published:

DOI: <http://doi.org/10.1111/pce.13660>

Terms of use:

Some rights reserved. The terms and conditions for the reuse of this version of the manuscript are specified in the publishing policy. For all terms of use and more information see the publisher's website.

(Article begins on next page)

This item was downloaded from IRIS Università di Bologna (<https://cris.unibo.it/>).
When citing, please refer to the published version.

Varotto Serena (Orcid ID: 0000-0001-5219-7157)

Epigenetic signatures of stress adaptation and flowering regulation in response to extended drought and recovery in *Zea mays*

Cristian Forestan^{1*}, Silvia Farinati¹, Federico Zambelli², Giulio Pavesi², Vincenzo Rossi³ and Serena Varotto^{1*}

1 Department of Agronomy Animals Food Natural Resources and Environment (DAFNAE), University of Padova, Viale dell'Università 16, 35020 Legnaro (Italy)

2 Department of Biosciences, University of Milan, Via Celoria 26, 20133 Milano (Italy)

3 CREA - Centro di Cerealicoltura e Colture Industriali (CREA-CI), Via Stezzano 24, 24126 Bergamo (Italy)

* **Corresponding authors:** Cristian Forestan (cristian.forestan@unipd.it) and Serena Varotto (serena.varotto@unipd.it)

Funding information:

This work was financially supported by special grants from the European Commission (FP7 Project KBBE 2009 226477 - "AENEAS": Acquired Environmental Epigenetics Advances: from Arabidopsis to maize), Italian CNR Flagship project EPIGEN the COST Action Impact of Nuclear Domains on Gene Expression and Plant Traits (INDEPTH, CA16212).

Abstract

During their lifespan, plants respond to a multitude of stressful factors. Dynamic changes in chromatin and concomitant transcriptional variations control stress response and adaptation, with epigenetic memory mechanisms integrating environmental conditions and appropriate developmental programs over the time. Here we analyzed transcriptome and genome-wide histone modifications of maize plants subjected to a mild and prolonged drought stress just

This article has been accepted for publication and undergone full peer review but has not been through the copyediting, typesetting, pagination and proofreading process which may lead to differences between this version and the Version of Record. Please cite this article as doi: 10.1002/pce.13660

before the flowering transition. Stress was followed by a complete recovery period to evaluate drought memory mechanisms. Three categories of stress-memory genes were identified: i) “transcriptional memory” genes, with stable transcriptional changes persisting after the recovery; ii) “epigenetic memory candidate” genes in which stress-induced chromatin changes persist longer than the stimulus, in absence of transcriptional changes; iii) “delayed memory” genes, not immediately affected by the stress, but perceiving and storing stress signal for a delayed response. This last memory mechanism is described for the first time in drought response. In addition, applied drought stress altered floral patterning, possibly by affecting expression and chromatin of flowering regulatory genes. Altogether, we provided a genome-wide map of the coordination between genes and chromatin marks utilized by plants to adapt to a stressful environment, describing how this serves as a backbone for setting stress memory.

Summary statement:

Dynamic analysis of transcriptomic and chromatin mark changes after prolonged mild drought stress and recovery period reveals different subsets of genes potentially involved in stress memory in maize.

Keywords

Zea mays, transcriptomics, drought stress, stress memory, histone modifications, ChIP-Seq

Acknowledgments

The authors would like to thank Prof. Zoya Avramova, Prof Hank Bass, Prof. Fiorella Lo Schiavo, Dr, Massimiliano Lauria and Dr. Nicola Carraro for critical reading of the manuscript and helpful comments, and Prof. Benedetto Ruperti for use of the microscope.

The authors declare that there is no conflict of interest regarding the publication of this article.

Author contributions

C.F., S.F. and S.V. designed and managed the study. C.F. S.F. and V.R performed the research. C.F F.Z and G.P analyzed the data. C.F., V.R. and S.V. conceived and wrote the manuscript with the contribution and the approval of all authors.

Introduction

Climate change is influencing rainfall patterns making them less predictable (Seager, Tzanova & Nakamura 2009; Cook, Anchukaitis, Touchan, Meko & Cook 2016) and with major constrains on water availability. Plants adopt specific strategies to cope with water scarcity and avoid drastic effect on their grown and development (Chinnusamy & Zhu 2009; Zhu 2016). Drought induces specific stress signaling pathways, usually related to hormones like abscisic acid (ABA), jasmonic acid (JA) and ethylene, resulting in production of proteins that prevent cellular damage (Tiwari, Lata, Chauhan, Prasad & Prasad 2017). Also regulatory proteins, including transcription and post-transcription factors, as well as kinases and phosphatases, and signaling molecule levels are altered by water stress (Nakashima, Yamaguchi-Shinozaki & Shinozaki 2014; Janiak, Kwaśniewski & Szarejko 2016; Haak *et al.* 2017). In addition, chromatin regulatory mechanisms have a fundamental role in spatio-temporal gene expression changes during stress response and adaptation (Asensi-Fabado, Amtmann & Perrella 2017). The presence of specific types of histone variants and histone post-translational modifications (PTMs), in combination with distinctive DNA methylation patterns, defines predominant chromatin states, with characteristic biochemical features and transcriptional potentials (Vergara & Gutierrez 2017). In stress response, chromatin dynamics

have been suggested to contribute to lasting changes in differential gene expression (type I transcriptional memory), or to variations in re-induction of gene expression (type II transcriptional memory). In type I memory, gene transcripts are maintained at high levels at the end of the stress and after a recovery period. In type II, the response to subsequent stress events is modified in comparison to the first response to the same stress cue (Bäurle 2018).

Some histone PTMs have been preferentially associated to stress response in different plant species (Avramova 2015; Haak *et al.* 2017). For instance, acetylation of histone H3 at lysine 9 (H3K9ac) is a chromatin mark found around gene Transcription Start Sites (TSSs) and closely correlated with transcription activation during plant development and differentiation (Wang *et al.* 2009; He *et al.* 2013; Du *et al.* 2013). Moreover, time-course analyses of histone modifications in plant tissues have shown dynamic changes of H3K9ac in response to environmental stimuli and stresses (Hu *et al.* 2012b; Zheng *et al.* 2016; Li *et al.* 2018).

In plants about 40% of the genes are also marked by H3K4me3, which is located predominantly on nucleosomes at the 5'-end of genes (Zhang, Bernatavichute, Cokus, Pellegrini & Jacobsen 2009; He *et al.* 2010; Hu *et al.* 2012a). Genes presenting this histone modification are actively transcribed, and H3K4me3 plays an important role in transcriptional regulation during development and in response and adaptation to environmental stresses (Kim *et al.* 2008; Wang *et al.* 2009; van Dijk *et al.* 2010; He *et al.* 2013; Song *et al.* 2015). Recently, H3K4me3 was linked to 'memory' both of drought and heat stress in plants (Ding, Fromm & Avramova 2012; Ding *et al.* 2013; Kim *et al.* 2012; Sani, Herzyk, Perrella, Colot & Amtmann 2013; Lamke, Brzezinka, Altmann & Bäurle 2016; Feng *et al.* 2016; Lamke & Bäurle 2017). After a first moderate stress treatment, H3K4me3 levels at the promoters of 'memory genes' increased. The increased H3K4me3 persists for several days, and contributes to higher transcriptional activation levels and stress tolerance upon a second stress treatment (Ding *et al.* 2012; Lamke *et al.* 2016).

In plants, H3K27me3 marked genes have very low expression levels and a high degree of tissue specificity, consistent with the function of H3K27me3 in maintaining gene repression during growth (Zhang *et al.* 2007; Turck *et al.* 2007; Wang *et al.* 2009; Lafos *et al.* 2011).

Despite the fact that many genes dynamically regulated in response to environmental cues are marked by H3K27me3 (Charron, He, Elling & Deng 2009; Li *et al.* 2013), H3K27me3 itself does not interfere with or inhibits their transcriptional activation (Kwon, Lee, Choi & Chung 2009; Liu, Fromm & Avramova 2014b; Liu, Ding, Fromm & Avramova 2014a).

By interfering with endogenous cues, drought stress can strongly influence plant reproductive development, including the transition from vegetative to inflorescence meristem and flower formation (Song, Ito & Imaizumi 2013; Kazan & Lyons 2016; Begcy & Dresselhaus 2018).

Depending on the species and timing, drought stress can both accelerate or inhibit the flowering process, as recently reviewed in Kazan and Lyons, 2016 and Takeno, 2016, and different genes are emerging as interconnecting regulators of floral development and drought responses in different plant species (Mishra & Panigrahi 2015; Galbiati *et al.* 2016; Hyun, Richter & Coupland 2017; Miao, Han, Zhang, Chen & Ma 2017). Investigating transcriptional and epigenetic mechanisms underlying plant response to drought stress is therefore essential for understanding and improving plant adaptation strategies to adverse environmental conditions.

Maize is highly susceptible to drought, especially during seedling, pre-flowering and grain filling stages (Bänziger & Araus 2007; Zheng *et al.* 2010). In this work we thus explore maize response to mild and prolonged drought stress and recovery, at both transcriptional and chromatin levels. We show that variations in gene expression are correlated to histone modification dynamics in stressed plants compared to control. In addition to genes transiently responding to drought stress at both transcriptional and chromatin level, three different subsets of memory genes were identified. The first subset of dehydration stress-responding

genes is characterized by transcriptional changes that persist after a complete recovery phase. The sustained alteration of transcript levels after stress relief illustrates a type I transcriptional memory response (expression of non-memory genes is rapidly restored to pre-stress levels at the end of the environmental cue, Bäurle, 2018). At many of these loci, we detected the ability of chromatin marks associated with genes to keep transcriptional potential for longer periods, providing a mechanism for the transcriptional memory responses observed. Second, we identified subsets of genes in which stress-responsive histone modifications persist for a longer time than the stimulus, even in absence of durable transcript level alterations. These marks represent putative epigenetic memory marks that could affect transcriptional performances of these “epigenetic memory candidate” genes when responding to subsequent stress, as previously demonstrated for H3K4me3 during recurring dehydration stresses in both *Arabidopsis* and maize seedlings (Ding *et al.* 2012, 2013, 2014). Third, for both transcript and histone modifications levels, we identified a category of genes not showing an immediate response to stress, but perceiving and storing stress signals for a delayed response, detectable only after the recovery stage. This category of “delayed memory” genes is enriched for TFs involved in flowering and inflorescences patterning and points to novel mechanisms for storing stress memory in plants. Finally, at phenotypic level, both a delay and alteration in male inflorescence development were observed consequently to drought treatment and recovery.

Altogether, stress-induced stable expression patterns and chromatin states may represent a coordinated strategy for plants to rapidly adapt to mild stressful environment and increase reproductive chances.

Materials and methods

Plant materials, stress protocol and tissue collection

The *Zea mays* B73 inbred line was used for transcriptome and chromatin immunoprecipitation sequencing (RNA-Seq and ChIP-Seq analyses, respectively). To apply drought stress, the plants were grown in pots in a greenhouse during spring-summer growing season (three independent experiments were performed in 2011 and 2012). Stress conditions and time points for collection of plant materials were chosen based on physiological parameters (biomass accumulation, CO₂ assimilation, stomatal conductance and quantum efficiency of photosystem II) as previously described in Morari *et al.*, 2015. Time course analysis during progressive dehydration indeed revealed that B73 plants start to perceive the stress after 4 days and then gradually decreased all physiological parameters, reaching a quasi-complete stomatal closure at the 10th day of treatment, while more than 4 days of recovery are necessary for a complete restoration of all the analyzed parameters. Plants were therefore regularly watered to pot capacity until the V5/V6 developmental stage, when dehydration treatment was applied: non-stressed plants (NS) were grown at a water content of 75% available water capacity, replenishing the water lost by evapotranspiration every day, while drought-stressed plants (WS) were watered replenishing only 60% of daily evapotranspiration to a minimum water content threshold of 25% of the available water capacity (Morari *et al.* 2015; Forestan *et al.* 2016). The treatment caused progressive shrivelling of WS plants starting from days 5-6 and well visible after 10 days of treatment (T0), when the youngest wrapped leaf (arrows in Figure 1A) was harvested from a subset of randomly selected plants. The other subset of plants was afterwards watered to pot capacity for seven days to recover from stress and the youngest wrapped leaf was then harvested from each plant (T7). In addition, samples were collected from a subset of stressed and control plants after 4 days of recovery (T4). Three biological replicates (R1, R2 and R3) were

produced; leaf samples of four-five plants for each combination of treatment per time-point per replicate were pooled together, flash-frozen in liquid nitrogen and stored at -80 °C. All plant materials were sampled between 11.00 AM and 1.00 PM, to avoid as much as possible diurnal variation in gene expression that would mask the stress effects.

RNA-Seq differential expression analysis

Transcriptome analysis was performed reanalysing previously produced RNA-Seq reads (Forestan *et al.* 2016), corresponding to control and stressed samples harvested at end of stress application (NST0 and WST0) and of the recovery period (NST7 and WST7). Total RNA extraction and processing, libraries preparation and sequencing on an Illumina HiSeq2000 platform, together with the bioinformatics analysis are therefore fully described in Forestan *et al.*, 2016. In brief, the sequenced reads were pre-processed for adapter clipping using Cutadapt 1.2.1 (Martin 2011) and then trimmed on low sequence quality bases and filtered from rRNA contaminant reads with ERNE-FILTER 1.2 (Fabbro, Scalabrin, Morgante & Giorgi 2013). High quality reads (Data S1) were mapped against the maize B73 reference genome (RefGen ZmB73 Assembly AGPv4 and Zea_mays.AGPv4.34.gtf Gramene transcript annotation; Jiao *et al.*, 2017) with Tophat 2.0.13 (Kim *et al.* 2013).

Raw read counts mapped on exonic regions of each gene were computed in both sequencing replicates (corresponding to biological replicates R1 and R2+R3, which were pooled and sequenced together) with HT-Seq count (Anders, Pyl & Huber 2015). Principal component analysis (PCA) of sequenced samples and replicates was performed in R 3.5.2 using the `prcomp()` function, and the PCA plot produced using `ggplot2` (Figure S1A; Wickham 2009; R Core Team 2017).

Normalized mean expression values (Reads Per Kilobase per Million mapped reads - RPKM) for each gene in the four samples were obtained using Cuffquant and Cuffnorm (Data S2),

while pairwise differential expression analyses were performed with Cuffdiff (Trapnell *et al.* 2013) selecting the following options: --multi-read-correct, --compatible-hits-norm, --dispersion-method per-condition and --library-norm-method quartile. Genes with log₂ fold change ratio $\geq |1|$ and FDR- adjusted p value ≤ 0.05 were considered as differentially expressed genes (DEGs; Data S3), while genes with test status = NOTEST or LOWDATA (roughly corresponding to RPKM <1 in all the conditions) were considered not expressed (Data S2). K-means clustering of DEGs (k=8) was performed using the Morpheus software (<https://software.broadinstitute.org/morpheus/>).

Gene Ontology (GO) enrichment and functional analysis

GO term enrichment was determined by comparing the number of GO terms in DEGs to the number of GO terms in the expressed genes via Blast2GO Enrichment Analysis - Fisher's Exact Test (Conesa & Gotz 2008) with default parameters and a critical cut-off value of false discovery rate ≤ 0.05 . Maize GO annotation was retrieved from maize-GAMER project (Wimalanathan, Friedberg, Andorf & Lawrence-Dill 2018).

Functional analysis of differential expression (DE) genes was done using MapMan (Thimm *et al.* 2004; Usadel *et al.* 2009): overrepresentation of categories was determined using Fisher's exact test with Benjamini-Hochberg corrected P-values. A cut-off value of 0.05 (corresponding to a Z-score ≥ 1.96) was applied to identify enriched categories.

Real-Time qRT-PCR expression analysis

Quantitative Real-Time PCR was used to confirm the expression of selected target genes and investigate their transcript level dynamics in the intermediate time-point after 4 days of recovery. Biological replicates were pooled together and total RNA was extracted using the RNeasy Plant Mini Kit (QiAgen) and subjected to on-column DNase treatment (QiAgen).

Before reverse transcription, total RNA concentration and purity were determined by measuring OD₂₆₀ and OD_{260/280} ratio, respectively, on a NanoDrop 2000c spectrophotometer (Thermo Scientific). cDNA synthesis was performed with the SuperScript III reverse transcriptase kit (Invitrogen). According to the manufacturer's instructions, 1 µg of total RNA was used as a template together with 1 µl oligo (dT) 12–18 (0.5 µg/µl – Invitrogen).

Quantitative Real-Time PCR expression analysis was performed using a StepOnePlus™ Real-Time PCR System (Applied Biosystems) and the FAST SYBR® GREEN PCR Master Mix (Thermo Fisher Scientific), following the manufacturer's guidelines. Melting curves analysis revealed a single amplification product in each reaction. Three replicates were carried out for each primer combination in each sample and a relative quantification of gene expression (normalized to GAPC2 transcript quantities) was performed with the StepOne Software 2.3 (Thermo Fisher Scientific), after determination of amplification efficiencies for each target gene (Pfaffl Method; Pfaffl, 2001). Primer sequences are reported in Data S8.

Isolation and immunoprecipitation of chromatin

Chromatin was extracted from the same four samples used for transcriptome analysis. For each sample, an equal amount of leaf material derived from each biological replicate was mixed and finely powdered with liquid nitrogen. Detailed methods for chromatin purification, immunoprecipitation, and antibodies used are fully provided in Methods S1.

ChIP-Seq assay and data analysis

For ChIP-Seq assay, a total of 12 ChIP libraries (4 samples X 3 Abs) and one control library representing whole chromatin (WC, obtained from the NST0 sample) were prepared using the Ovation Ultralow Library System kit (Nugen) according to the manufacturer's

instructions. Each library was prepared pooling together the DNA obtained from three independent immuno-precipitation experiments. Illumina sequencing of the ChIP libraries was performed at the Institute of Applied Genomics (Udine, Italy) on an HiSeq2000 platform with a multiplex level of 4, producing on average 40 million of 50 bp single end reads per library. For the WC control library, 160 million of 50 bp single end reads were produced (Data S1).

FastQC 0.10.1 software was used for quality control, and reads were manually trimmed by 5 bp at the 3' end. Mapping was performed on the RefGen ZmB73 Assembly AGPv4 genome using bowtie2 (Langmead & Salzberg 2012) allowing at most 3 substitutions per read and no indels. Only reads mapping uniquely on the genome were kept for downstream analyses.

ChIP-Seq enrichment over genic loci was calculated with deepTools2 (Ramírez *et al.* 2016), using the *Zea_mays*.AGPv4.34.gtf Gramene gene models (Figure S5). Based on mapped read distribution profiles, read counts for H3K9ac and H3K4me3 were computed for each gene in each sample by considering the 1 Kb region downstream of annotated transcription start sites (TSS), while for H3K27me3 the whole gene transcribed region was considered (raw read counts are reported in Data S4). Normalized histone modification levels for each annotated gene in each sample were defined as RPM (Reads Per Million of reads) for H3K4me3 and H3K9ac, and RPKM (Reads per Million per Kilobase) for H3K27me3. To analyze multiple ChIP-Seq datasets in different biological conditions, principal component analysis (PCA) was performed in R 3.5.2 using the `prcomp()` function, and the corresponding plot was produced with the `ggplot2` package (Figure S1B; Wickham 2009; R Core Team 2017). To identify genes significantly enriched for a ChIP-Seq with respect to the WC control, multiple $2 \times 2 \chi^2$ (Chi-square) tests were performed, taking into account the number of reads falling within a region in the ChIP-Seq, the overall number of mapped reads of the ChIP-Seq, the number of reads in the region in the control, the overall number of reads mapped in the

control. This method thus takes into account both the relative enrichment for each gene in the ChIP versus the WC, and the relative abundance of the gene in each sample (raw number of mapped reads assigned to each gene versus the overall number of mapped reads of the experiment). Genes passing a strict Bonferroni-corrected p-value threshold of 1×10^{-6} were considered positive. H3K4me3 and H3K9ac histone modifications were confirmed to be positively associated to transcription, while H3K27me3 enrichment was associated to transcriptional repression (Table S2, Figure S6).

Genes displaying a significant variation of enrichment for each histone mark during the time-course of the stress and recovery application were similarly identified applying $2 \times 2 \chi^2$ tests in pairwise comparisons among the four samples. In this case, only the set of the genes previously identified as significantly enriched for each histone mark compared to WC control were considered, and those passing a p-value threshold of 1×10^{-2} were defined as differentially marked genes (DMGs). For representing results, p-values of χ^2 tests were \log_{10} transformed, and positive or negative signs were added to indicate the direction of variation of histone mark enrichment (Data S5-7). Hierarchical clustering of DMGs was performed using the Morpheus software (<https://software.broadinstitute.org/morpheus/>) and displayed as a heat map.

As control, genes significantly enriched for H3K4me3 and H3K9ac with respect to the WC control were analyzed also by considering reads mapping on the 1 Kb region upstream of annotated TSSs (thus roughly including the proximal promoters). Following this approach, a substantially lower number of enriched genes were identified for each modification, and a weaker association between enrichment for these activating marks and gene expression could be detected (Table S2). Furthermore, when used for DMGs identification, H3K4me3 and H3K9ac level changes in the promoter upstream region were not correlated to stress-induced gene expression variations (data not shown).

Microscopic analysis

To evaluate the effect of drought stress on floral transition and inflorescence development, SAMs and male inflorescences were dissected from control and stressed plants during the ten days of stress treatment and during the recovery period. The developmental stage of SAMs and inflorescences was determined using the binocular microscope Zeiss SteREO Lumar.V12. Inflorescence phenotypes were evaluated at anthesis stage, too.

Accepted Article

Results

Leaf transcriptome analysis reveals specific targets of mild drought stress and different gene expression dynamics after water recovery

To identify global transcriptomic changes we performed RNA sequencing (RNA-Seq) on the youngest wrapped leaf of maize B73 inbred plants. Immature wrapped leaves were used because they integrate environmental and endogenous cues driving plant development better than mature leaves (Colasanti, Yuan & Sundaresan 1998; Hempel, Welch & Feldman 2000; Meng, Muszynski & Danilevskaya 2011) and to, at least partially, exclude the primary large impact of water stress on photosynthesis gene expression (Chaves, Flexas & Pinheiro 2009). Plants at the V5/V6 developmental stage were subjected to a progressive, mild dehydration stress for ten days (WST0) followed by seven days of recovery (WST7). Control plants, continuously grown in the absence of stress were sampled at the same time points (NST0 and NST7, respectively; Figure 1A).

RNA-Seq transcriptome analysis revealed 1,957 and 794 genes down- and up-regulated by drought, respectively (WST0 vs NST0; Table 1 and Table S1), indicating that drought stress has a prevalent repressive impact on gene expression. Comparison between stressed plants and plants after stress recovery (WST7 vs WST0) identified 633 differentially expressed genes (DEGs); about the 80% of these genes were also included among DEGs in WST0 vs NST0, but with opposite direction of the detected change (Table 1). Comparison between NST7 vs WST7 samples showed only 36 differentially expressed genes, while none were singled out in the pairwise comparison between control plants at different sampling time points (NST0 vs NST7; Table S1 and Data S3).

MapMan (Thimm *et al.* 2004; Usadel *et al.* 2009) and Gene Ontology (GO) enrichment analyses displayed an over-representation for functional categories related to “stress response”, “abscisic acid metabolism”, “regulation of transcription” and “secondary

metabolism” among genes up-regulated in WST0 compared to NST0 (Figures 1B and S2).

Stress down-regulated genes showed a strong enrichment in many growth- and development-related functional terms. The same GO terms were also enriched in WST7 vs WST0 DEGs, but with a reversed pattern, since they mainly represent genes transcriptionally reset following the recovery period. Among the few NST7 vs WST7 DEGs no functional terms were significantly enriched, even if the GO analysis displayed transcription factors as over-represented annotations of the NST7 up-regulated genes.

These results indicate that application of mild drought stress affects expression of many genes involved in various biological processes and that their original expression level is generally restored after re-watering.

To better evaluate gene expression dynamics after stress application and recovery, clustering of genes differentially expressed in at least one pairwise comparison (2,895 genes) was performed (Figure 1C). GO enrichment analysis was then applied to genes included in each cluster (Figures S3-S4). Stress-downregulated genes (i.e. with lower mRNA level in WST0 vs NST0) belonged to clusters 1, 2, and 3 (1,913 genes in total, enriched in many functional terms): all three clusters indicate that down-regulation is almost completely reversed after the recovery period. Stress up-regulated genes (i.e. with higher mRNA level in WST0 vs NST0) were split into three different clusters as well. While clusters 5 and 6 (718 genes in total, enriched in stress response correlated GOs) contain genes transiently induced in WST0 and with low mRNA levels in all other samples, genes in cluster 7 (130 genes, enriched in stress and hormone associated GOs) maintain high mRNA levels also after stress removal and recovery. Cluster 8 contains 21 genes with higher transcript level in NST7 compared to WST7 and includes several transcription factors involved in development and flowering regulation. Finally, cluster 4 contains 113 genes only weakly altered in WST0 vs NST0, but expressed at higher levels in WST7 compared to WST0.

In conclusion, under our experimental conditions, 130 genes up-regulated by drought maintain a relatively higher mRNA level during recovery, representing drought stress type I transcriptional memory genes. Conversely, the expression of almost all stress down-regulated genes is restored to a level similar to not stressed plants. In addition, clustering analysis identified DEGs with substantial differences in mRNA level between NST0 and NST7, not identified by pairwise comparisons, also indicating that these developmentally regulated DEGs differently respond to the drought stress. This group of genes not showing an immediate response to stress, but perceiving and storing stress signal for a delayed response represents a new form of stress transcriptional memory.

H3K4me3, H3K9ac, and H3K27me3 level differentially correlate with gene expression and are affected by drought

The effect of drought stress on chromatin and its correlation with gene expression was investigated by analyzing the level of histone modifications by ChIP-Seq. Histone modifications classically associated with transcriptional activation (histone H3 lysine 9 acetylation: H3K9ac and histone H3 lysine 4 tri-methylation: H3K4me3) and repression (histone H3 lysine 27 tri-methylation: H3K27me3) previously involved in plant drought stress response were selected for this purpose (Avramova 2015; Haak *et al.* 2017).

ChIP-Seq read distribution over genic loci showed H3K4me3 and H3K9ac enrichment in the region downstream of the transcription start site (TSS; Figure S5), while H3K27me3 was uniformly distributed over the transcribed region. Genes not expressed are characterized by H3K27me3 and low H3K4me3 and H3K9ac level, while the increase of gene expression correlates with a progressive increase of H3K4me3 and H3K9ac and decrease of H3K27me3 levels (Table S3 and Figure S6A-C).

The impact of drought stress on chromatin features was estimated by identifying genes with a statistically significant change in ChIP-Seq enrichment in pairwise comparisons. For each histone mark, differentially marked genes (DMGs) were identified applying $2 \times 2 \chi^2$ tests (see Materials and Methods; Table S3, Figure S6D and Data S5-7). The largest number of H3K4me3 DMGs was observed in WST7 vs WST0 with a comparable fraction of genes showing methylation gain or loss. The highest number of genes with change in H3K9ac were detected in WST0 vs NST0 comparison, with the larger part of them exhibiting stress-induced H3K9ac reduction. The majority of genes with changes in H3K27me3 were found by comparing NST7 vs WST7 samples, most of which increased H3K27me3 level in WST7. GO enrichment analysis of DMGs is reported in Figure S7.

Comparisons between DMGs and DEGs identified in WST0 vs NST0 revealed a positive correlation between changes in H3K4me3 and gene expression (Mann-Whitney test $p < 0.01$ in Figure 2A; Figure S8A). The 25% of the 1,044 DMGs showing an increase in H3K4me3 were up-regulated DEGs while only the 4% of them were down-regulated (Figure 2A). Similarly, 36% of the DMGs with a reduction of H3K4me3 in WST0 were down-regulated by the stress, against the 0.7% that were up-regulated. A similar correlation was found for H3K9ac (Figures 2C and S8C). Drought-induced changes in H3K4me3 and H3K9ac marks mainly occurred on distinct subsets of genes. However, DMGs for both marks displayed a higher percentage of differentially expressed genes compared to DMGs in only one mark (Figure 2G-H). Regarding H3K27me3, no correlation with gene expression variation was found: indeed, response to drought mainly induces a decrease of H3K27me3 in both stress up- and down-regulated genes (Figures 2E and S8E).

In the WST7 vs WST0 comparison a weaker correlation between H3K4me3 and gene expression during stress recovery was detected: only down-regulated genes showed a significant global decrease in H3K4me3 level (Mann-Whitney test $p < 0.01$ in Figure 2B;

Figure S8B). The 12.7% of the 1,706 DMGs with H3K4me3 decrease were indeed down-regulated, while only 6.7% of the 1,179 genes with H3K4me3 increase showed a corresponding increase of expression (Figure 2B). Also for H3K9ac both overlap and correlation between DMGs and DEGs are weaker than those observed in WST0 vs NST0 (Figures 2D and S8D).

Comparison of control and stressed plants at the end of the recovery period (NST7 vs WST7) further indicated that recovery from the stress had a reduced correlation between H3K4me3 or H3K9ac level changes and variations in gene expression. Approximately 90% of H3K4me3 or H3K9ac DMGs did not show change in expression (Figure S9A and D) and no statistically significant correlation between DMGs and DEGs was found (Figure S9B-C and S9E-F).

H3K27me3 analysis during the recovery from the stress showed a reversion of the previously observed decrease of H3K27me3 level in WST0 (Figure 2F), and its increase in DMGs during recovery is even more evident in NST7 vs WST7 comparison, that is the pairwise comparison with the higher number of H3K27me3 DMGs (Figures S6D and S9G; Table S3). However, in both WST7/WST0 and NST7/WST7 comparisons, a correlation with gene expression variation was not observed (Figures 2F, S8F and S9H-I).

In summary, these results indicate that a positive correlation between gene expression and H3K4me3/H3K9ac variation mainly occurred following stress treatment. Furthermore, H3K27me3 changes do not correlate with stress-induced gene expression variations at all. However, stress induced histone modification changes may act as an epigenetic blueprint, independently of or without an immediate effect on gene expression. In fact, changes in levels for one or more histone modifications may be the mechanistic strategy for setting, storing and transmitting memory of stress experience during plant development.

Drought induced histone modification can be maintained or reset during stress recovery period

To analyze the potential role of DMGs and for evaluating the dynamic of each chromatin modification over the course of stress and recovery, we performed hierarchical clustering analyses of genes on the basis of their enrichment profiles across the samples. We manually defined 9 clusters for H3K4me3, 12 for H3K9ac, and 8 for H3K27me3 (Table 2, Figures 3, 4 S10, S12 and S14). Some of these profiles belonged into two well-defined dynamic categories: i) histone modification levels altered after stress treatment (WST0 vs NST0, hence these categories were named ST and can exhibit gain or loss in a given histone mark), and ii) delayed histone changes that occurred during stress recovery (WST7 vs NST7, hence these categories were named SR with histone mark gain or loss). Additional clusters with less defined categories or characterized by differences in histone modification between time-points, independently of the stress treatment, are not further discussed here.

ST gain and loss groups displayed the direct stress effect at WST0. These groups have been further sub-grouped by considering whether the stress-induced variation is maintained (ST Stable) or reset to initial values (ST Transient) after the recovery period. For H3K4me3, ST Transient Gain and Loss clusters were the categories with the larger number of genes (Figures 3 and S10), indicating a prevalent reversion of the H3K4me3 stress-induced changes after re-watering. On the other hand, ST Gain Stable cluster (71 genes of which 26 share “stress response” as GO annotation) and ST Loss Stable group (350 genes with over-represented GO terms like “cell cycle”, “shoot growth”, “flower development”) include genes with stress induced H3K4me3 changes maintained also at WST7 (Figures 3, S10 and S11). Four similar ST groups were found for H3K9ac (Figures 4, S12 and S13), but containing a smaller number of DMGs. Several H3K9ac mixed profiles were indeed identified and could not be classified as ST targets.

Only two ST clusters (Gain Transient and Gain Stable) were found for H3K27me3 (Figure S14), whereas more than a half of H3K27me3 DMGs was included in two SR clusters Gain and Loss. In SR groups, DMGs detected after the stress recovery by comparing stressed and not-stressed plants are included. Hence, SR groups are likely to represent histone modification changes directed both by stress and plant developmental program. SR clusters for H3K9ac and H3K4me3 DMGs were also identified (Figures 3, 4, S10 and S12), and many development-related GO terms are commonly over-represented in H3K4me3 SR Loss and H3K27me3 SR Gain clusters (Figures S11 and S15).

Genes included in each cluster were further analyzed for changes in their mRNA levels.

According to above results, a positive correlation between H3K4me3 or H3K9ac and gene expression was observed at the end of stress treatment, while only H3K4me3 positively correlated with expression after the recovery period (Figures 3 and 4). H3K4me3 Gain

Transient genes exhibited significantly higher expression in WST7 compared to NST7

(Mann-Whitney test $p < 0.001$), while the higher average expression of Gain Stable genes in

WST7 was not statistically significant (Mann Whitney test $p = 0.081$), probably due to the

low number of genes analyzed ($n = 53$). Lower average expression levels at WST7 compared

to NST7 were detected at the Loss Transient cluster genes but not at the Loss Stable ones. It

is worth noting that lower expression in WST7 compared to NST7 characterizes also the

H3K9ac ST Loss Transient genes (Mann-Whitney test $p < 0.01$, Figure 4), and those showing

a ST Transient Gain of H3K27me3 (Mann-Whitney test $p < 0.001$, Figure S14).

Low H3K4me3 level in SR clusters (SR Loss cluster) is associated with a significantly lower

average gene expression at WST7 compared to NST7 (Mann-Whitney test $p < 0.001$; Figure

3). Correlation between H3K9ac and H3K27me3 level and gene expression in SR clusters is

less clear and predictable (Figures 4 and S14).

These analyses identified distinct clusters containing genes, where stress-induced variations of histone modification levels persist after stress removal, or where the variation is detectable only after the recovery as a delayed stress effect. Among analyzed histone marks, H3K4me3 levels can better correlate to changes in gene expression than H3K9ac and H3K27me3.

Identification of potential drought stress memory targets

At molecular level, type I transcriptional stress memory is often mediated by chromatin modifications (Avramova 2015; Friedrich, Faivre, Bäurle & Schubert 2018; Bäurle 2018). To identify potential “epitargets” of stress response, we focused on gene loci showing stress induced transcriptional and chromatin variations, which are maintained after the 7 days of recovery. We found that members of well-characterized dehydration responsive gene families, such as AP2/EREBP, NAC and WRKY transcription factors (Chen & Zhu 2004; Janiak *et al.* 2016; Joshi *et al.* 2016) are included in DEGs induced by stress (WST0 vs NST0; Figure 1B) and some of them maintain stress-induced transcriptional and/or histone modification levels after stress removal (included in Cluster 7; Figure 1C). For example, of twelve stress up-regulated WRKYs, ten maintained higher mRNA levels in WST7 compared to NST7 (Figure 5A), with *WRKY104* (*Zm00001d020495*) also showing a stable increase in H3K4me3 and H3K9ac. Stress transcriptional memory was observed for *EREB172* and *EREB198* (*Zm00001d031796* and *Zm00001d002762*, respectively) and *NAC25*, *NAC49* and *NAC109*, but at these loci only transient changes in H3K4me3 or H3K9ac were observed (Figure 5B-C).

Another group of stress-induced genes includes genes involved in abscisic acid (ABA) synthesis and signaling pathways (Figures 1B and 5D). For example, *Zm00001d003512*, encoding a chloroplastic zeaxanthin epoxidase involved in ABA synthesis, maintained transcriptional up-regulation after stress removal, even if associated with a transient increase

of H3K4me3 (Figure 5D). 9-cis-epoxycarotenoid dioxygenase (NCED) catalyzes the control point reaction in ABA biosynthesis in leaf (Tan, Schwartz, Zeevaart & McCarty 1997; Seo & Koshiba 2002). Of four NCED genes strongly up-regulated after ten days of stress application, *NCED6* and *NCED8* showed sustained expression after stress recovery (included in Cluster 7; Figure 1C), while *VP14* and *NCED 5* represented non memory genes (Figure 5D). After recovery, the high H3K4me3 levels at *NCED6* (*Zm00001d051556*) locus reflect its transcriptional activity, while the recovery period determined the reset both of H3K4me3 and expression levels at *VP14* (*Zm00001d033222*) locus (Figure 5D-E).

These results point at the several transcription factors and ABA biosynthetic genes as dehydration stress “memory” genes. By controlling the transcriptional potential of some of them stable chromatin marks, provide a mechanism for the transcriptional memory responses of *WRKY104*, *EREB172* and *NCED6*.

Delayed responsive genes represent a novel mechanism for storing stress memory

Besides the above described stress responsive TFs, GO enrichment and curated annotations revealed many genes involved in development and flowering regulation among both DEGs and DMGs (Figures S2, S4, S11 and S15). We found two paralogous genes encoding MADS box transcriptional regulators that were differentially expressed after stress removal (i.e. NST7 vs WST7). *ZmMADS4* (*ZMM4*; *Zm00001d034045*) and *ZmMADS15* (*ZMM15*, *Zm00001d013259*) were indeed included in the Cluster 8 of developmentally regulated, stress-affected DEGs (Figure 1C), being expressed exclusively at T7 in leaves of plants that did not experience the stress. The transcriptional rise of *ZmMADS4* at NST7 is associated with the concomitant increase of H3K4me3 and decrease of H3K27me3, while both histone modifications were altered by the experienced drought stress. *ZmMADS4* was indeed included in the H3K27me3 ST Gain transient and H3K4me3 SR Loss clusters because,

compared to control, drought caused a transient increase of H3K27me3 level at WST0 and lower H3K4me3 level at WST7 compared to NST7 (Figure 6; Table 3). Differently to *ZmMADS4*, *ZmMADS15* was included in the H3K27me3 SR Gain cluster, exhibiting a statistically significant increase of H3K27me3 level, together with decreased H3K4me3, in WST7 vs NST7 (Figure 6; Table 3).

To better evaluate the dynamics of *ZmMADS4* and *ZmMADS15* expression after stress removal, we estimated their transcript level at an intermediate time-point during the recovery period (four days: NST4 and WST4). Results showed that mRNA level of both genes are not affected by drought at T0 and T4, but only at T7 (Figure 6B). All our observations indicate that, in not stressed plants, *ZmMADS4* and *ZmMADS15* increase their expression at a developmental stage close to T7 and this correlates with a variation of active and repressive histone marks. Drought affects their developmentally-related expression increase by impairing accumulation of active and reduction of repressive histone marks at T7. Hence *ZmMADS4* and *ZmMADS15* are stress targets that perceive and record the stress event, but transcriptional response is probably delayed until plant reaches a specific developmental stage, in a new type of stress transcriptional memory.

Drought stress impacts mRNA and histone mark levels at genes associated to inflorescence patterning, resulting in delay and alteration of male inflorescence development

GO enrichment and curated annotations of DEGs and DMGs also revealed that 37 genes differentially expressed in WST0 vs NST0 leaves are regulators of flowering transition and inflorescences patterning (Minow et al., 2018; Tenailon et al., 2018; Figure 6A, Table 3 and references included). They include *IDI*, the master regulator of the transition to flowering, which is downregulated by drought, while the expression of the florigenic gene *ZCN8*, as

well as mRNA level of other genes acting downstream of the *ID1* regulatory pathway (i.e. *DLF1* and *MADS1*) were not affected by drought. Among floral regulators down-regulated by drought there were three SQUAMOSA-PROMOTER BINDING (SPB) protein coding genes (*TASSEL SHEAT4 - TSH4*, *UNBRANCHED2 - UB2*, and *UB3*; Figure 6A and Table 3), which have critical roles in regulating maize flowering time and inflorescences architecture. For *TSH4*, expression down-regulation correlated with a transient decrease of H3K4me3. Transient down-regulation and stable decrease of H3K4me3 level was instead detected for *ROTTEN EAR (RTE)* locus, encoding for a boron transporter involved in inflorescence patterning. Transient drought induced decrease of mRNA levels also occurred in two genes involved in the control of flowering through the gibberellin homeostasis regulation (*GIBBERELLIN 2-OXIDASE7 - GA2ox7*) and signaling pathway (*DWARF8 - D8*). Drought induced up-regulation of genes involved in circadian clock and photoperiod floral regulatory pathway. For example, transient up-regulation was reported for two *FLAVIN-BINDING, KELCH REPEAT, F BOX (FKF1 and FKF2)* blue light photoreceptors, *CONSTANS-like 15 (COL15)*, and for the flowering repressor *GIGANTEA2 (GI2)*, with the latter also exhibiting transient increase of H3K9ac level.

To evaluate the impact of these drought-induced chromatin and transcriptional alterations on inflorescence patterning, SAMs and male inflorescences were dissected from control and stressed plants during stress treatment and recovery. Microscope imaging of plant SAMs at V5/V6 leaf stage revealed that the progressive dehydration stress started exactly in concomitance with vegetative to reproductive transition at the shoot meristem (Figure 7A). After 7 days of stress application, tassel primordia of stressed plants were shorter, with fewer and smaller branch primordia compared to control plants (Figure 7B-C). The differences in primordium and branch size were even more evident after ten days of stress application (Figure 7D-E) and it also persisted during the recovery (Figure 7H-I). At the end of the stress

application, close-up observation of the tassel primordium tip revealed the indeterminacy of meristem compared with control developing inflorescences, indicating a delay in inflorescence development (Figure 7F-G). Indeterminacy of inflorescence meristem was maintained in stressed plants after 4 days of recovery (Figure 7J-K), and, at the end of recovery, the alterations in size and number of male inflorescence branches were even more evident (Figure 7L) and persisted until anthesis (Figure 7M-N). The developmental delay was also maintained at full maturity: the experienced drought stress determined a 5-days delay in flowering time that affected only the male inflorescence (first pollen shed; T-test $p < 0.05$), without altering the time of silking or the ear phenotype.

These observations provide evidence that mild drought stress impairs male inflorescence patterning.

Discussion

In this work we presented a global analysis of transcriptome and of selected histone modifications in maize plants subjected to a progressive, dehydration stress and a full recovery period that mimics the field conditions during the pre-flowering stage. Maize response to water stress varies accordingly to both the plant developmental stage and stress timing and intensity (Blum 2014). In field conditions, water stresses are often transient and the recovery phase following stress removal is critical for stress impact on maize yield. However, in studies published so far, osmotic stress has been mostly simulated *in vitro* by the addition of polyethylene glycol (PEG) or, when plants have been grown in soil, they have been sampled at seedling stage soon after hours of air-drying or a few days of drought treatment (Jia *et al.* 2006; Lu *et al.* 2011; Shan *et al.* 2013; Ding *et al.* 2014; Opitz *et al.* 2014; Wu, Ning, Zhang, Wu & Wang 2017). In addition, only a few studies have addressed the genetic and epigenetic regulation of traits for tolerance/susceptibility to drought

considering recovery as a real component of environmental challenges in the field (Zhang, Lei, Lai, Zhao & Song 2018).

Dynamics and memory of drought induced transcriptional variations

Transcriptome analysis confirms the negative impact of the imposed drought stress on leaf growth and development (Zhang *et al.* 2018): among the 2,751 DEGs identified at the end of the stress treatment, the 1,957 stress down-regulated genes are indeed enriched in functional terms associated to cell cycle regulation, growth and cell wall biosynthesis, indicating the inhibition of both cell division and expansion rates during water deprivation. Many of these genes were previously found down-regulated in the maize leaf growth zone after mild and severe drought stresses (Granier, Inzé & Tardieu 2000; Avramova *et al.* 2015). Our analysis indicates that their drought-induced down-regulation is transient in our experimental conditions.

The stress response involves the up-regulation of well characterized transcription factors (TFs) and genes mediating hormone, secondary and oxidative metabolism. For a subgroup of these up-regulated genes, e.g. members of AP2/EREBP, NAC and WRKY TFs families, our analysis showed higher mRNA levels also after 7 days of recovery, indicating they represent type I transcriptional memory genes.

Abscisic acid (ABA) is often described as the stress hormone because plants adjust ABA levels in response to different abiotic stresses (Tan *et al.* 1997, 2003; Iuchi *et al.* 2001; Seo & Koshiba 2002; Tuteja 2007). In our study, the expression levels of the genes catalyzing all the steps of ABA biosynthesis (*ZEP1*, four *NCEDs* and two *AOs*) were significantly higher in response to water scarcity (WST0 vs NST0) and for *ZEP1* and *NCED6* higher mRNA levels were detected in WST7 compared to NST7, indicating type I transcriptional memory.

Type II dehydration stress memory genes have been previously investigated in Arabidopsis and maize in plants subjected to multiple short-term stresses, 2 hours dehydration stress followed by 22 h of full rehydration (Ding *et al.* 2012, 2013, 2014; Virilouvet *et al.* 2018). Despite the completely different experimental set-up (short-term air exposure vs ten days progressive drought stress) and tissues analyzed (2 week old seedlings vs immature wrapped leaf of V7 plants), similarities could be found between the subset of genes responding to different water withdrawal stresses in maize. For example, the 40% of genes up-regulated in our assay increase significantly expression also during repetitive dehydration stresses, while only the 10% of overlap was found between stress-repressed genes in the two assays. Remarkably, *NCED6* was classified among the delayed response memory genes, i.e. genes that do not alter expression after the first stress exposure, but significantly increases their expression after subsequent stresses (Virilouvet *et al.* 2018). Conversely, *VP14* up-regulation was detected only during the first stress exposure, confirming the different transcriptional regulation of the two paralogs.

Histone modification can act as an epigenetic blueprint for remembering stress experience during plant development

The ability of chromatin to undergo both dynamic and stable structure changes in response to stress has been considered a mechanism for regulation of primary stress response (Asensi-Fabado *et al.* 2017; Haak *et al.* 2017) and memory storage (Kim *et al.* 2012; Sani *et al.* 2013; Avramova 2015; Lamke & Baurle 2017; Friedrich *et al.* 2018; Bäurle 2018). In line with previous works, our results indicated a direct correlation between the presence of both H3K4me3 and H3K9ac and gene expression after stress application. When comparing WST0 and NST0, differentially expressed genes are well associated to differing amounts of both marks, but it is quite surprising that only 25 - 30% of the genes with elevated H3K4me3 or

H3K9ac levels were concomitantly significantly more transcribed (the same percentages applied to genes with mark and transcriptional levels decrease). Given the long progressive stress application, these altered chromatin mark levels could represent the remnants of modification changes associated to the early stress transcriptional response.

Correlation between activating histone marks and expression levels decreases after the recovery from the stress (WST7 vs WST0 comparison). Conversely, H3K27me3 repressive mark changes are not correlated at all to stress-responsive gene expression, in good agreement with previous studies on dehydration stress in *Arabidopsis* (Liu *et al.* 2014b a) . In contrast to its well-known role as a chromatin repressive mechanism at developmentally regulated genes, the authors demonstrated that presence of H3K27me3 did not prevent transcription from the dehydration stress responding genes, and H3K27me3 levels are not correlated with transcriptionally active/inactive gene state.

While a large part of the H3K4me3 and H3K9ac variations are reversed during the recovery, the maintenance of these marks in WST7 have been associated to the transcriptional memory of *NCED6* and some of the previously described TF gene family members (*WRKY104* and *EREB172*), revealing the chromatin component at the base of their stress transcriptional memory.

Nevertheless, considering the whole set of genes presenting stable levels of these chromatin marks (ST Gain Stable and Loss Stable clusters), a sustained transcriptional memory is not clearly detectable. This is not surprising for at least two reasons. First, even if proactive and protective to a subsequent stress, transcriptional memory is expensive for plants (Crisp, Ganguly, Eichten, Borevitz & Pogson 2016): histone marks could instead provide faster or stronger responses following a subsequent stress. The second aspect that must be taken into account is the impact of the nature and length of the experienced stress on the memory duration, together with the possible different duration of transcriptional and chromatin

memories. In *Arabidopsis*, dehydration stress transcriptional memory persists for 5-7 days and its loss coincides with the loss of the elevated levels of H3K4me3 at the memorized genes (Ding *et al.* 2012; Avramova 2015), while H3K4me3 and H3K27me3 changes induced by salinity hyperosmotic priming can be sustained for 10 days (Sani *et al.* 2013).

Remarkably, the 60-75% of the genes in each of the H3K4me3 and H3K9ac ST Stable clusters did not display significant variation of expression neither in the WST0 vs NST0 comparison. These stable histone marks could therefore store for long time the information about the early phases of stress response as previously discussed, allowing the plant to better adapt to a mild stressful environment and/or to respond faster or more efficiently to a recurrent stress exposure. Only the study of the impact of these stable histone marks on transcriptional regulation in subsequent stresses could resolve their nature of “epigenetic memory candidate”. In this perspective, our long-lasting experimental set-up scarcely adapts to investigate their role during a recurrent stress exposure. However, our results suggest that further investigations on the ABA role in drought memory establishment and maintenance could be useful to overcome this constrain: once investigated the ability of ABA to mimic the highlighted drought stress memory response, focused hormone applications could be used to prime maize plants before true drought stress application.

Our integrated data analysis also identified many genes with stress-induced increase in both mRNA and H3K4me3 or H3K9ac levels that, after re-watering and recovery, only maintain a sustained expression. The reversion of H3K4me3/H3K9ac levels at these loci after recovery does not exclude that other different histone modifications or “non-epigenetic” regulatory mechanisms are associated to their transcriptional memory.

Interestingly, genes with delayed chromatin mark changes (SR Clusters) outline a new type of stress-induced memory. These chromatin changes could represent the epigenome landscape remodeling necessary for restoring metabolic homeostasis or could be necessary to

modulate the plant proper developmental program accordingly to the experienced stress. Our results support the view that delayed changes in H3K4me3 and H3K27me3 levels might act as a double epigenetic lock to impair the transcriptional activation of *ZmMADS4* and *ZmMADS15* in the leaves of plants that experience the stress. *MADS4* and its closely related paralog *MADS15* represent indeed floral meristem integrator that promotes floral transition and inflorescence development, but they are also detectable in vegetative organs (Danilevskaya *et al.* 2008; Tenailon *et al.* 2018). Their expression, activated by the ZCN8-DFL1 complex but also by the ID1 direct autonomous path (Figure 6B), increases in the apex and leaves after floral transition and during inflorescence development, but up to now no information is available on their downstream targets and on their transcriptional regulation in maize leaf (Danilevskaya *et al.* 2008; Dong *et al.* 2012). Based on our results, in developing leaves H3K4me3 and H3K27me histone marks are involved in the transcriptional activation of both paralogs and water withdrawal impairs both mRNA and chromatin mark levels. The importance of H3K27me3/H3K4me3 ratio in gene expression reprogramming in the apical meristem during transition to flowering and flower development was previously highlighted in Arabidopsis, rice and brachypodium (Liu *et al.* 2015; You *et al.* 2017; Huan, Mao, Chong & Zhang 2018). The simultaneous presence of the active and the repressive modifications, and associated complexes, helps to maintain these “bivalent” loci in a state that is both responsive to developmental cues and at the same time insensitive to subthreshold noise (Voigt, Tee & Reinberg 2013; Liu *et al.* 2014b, 2015; You *et al.* 2017; Qian *et al.* 2018). For example, during Arabidopsis early flower morphogenesis, gene expression activation is predominantly accompanied by H3K4me3 increase, with a subsequent decline of H3K27me3 mark (Engelhorn *et al.* 2017). However, till now no report has documented a “bivalent”, stress-responding, H3K4me3/H3K27me3 regulation in the leaf for loci controlling inflorescence development. Further investigations are therefore necessary to dissect at

mechanistic level the role of drought stress on MADS4/MADS15 transcription and chromatin regulation, also considering that *MADS4* and *MADS15* expression was altered in leaves of maize epiregulator mutants *required to maintain repression6 (rmr6)* and *histone deacetylase 108 (hda108)* that were recently analyzed (Forestan *et al.* 2017, 2018).

Drought stress impacts on flowering and inflorescence development

Several studies evidenced that plants could alter flowering time in response to stress condition and it has been recently proposed that plants promote or inhibit flowering as an evolutionary strategy to maximize the chances of reproduction. Under a gradual mild stress, flowering is generally delayed, while under a strong, terminal stress, flowering is promoted to ensure reproduction before succumbing (Kazan & Lyons 2016; Takeno 2016). Our phenotypic analysis shown that, when stress treatment initiation is contemporary to meristem floral transition, drought affects male inflorescence development (Figure 7), delaying flowering time.

Drought perturbed the expression of many floral regulators and for some of them this alteration is well correlated to a loss in H3K4me3. One could argue that the observed expression and histone changes could be due to the observed delay in inflorescence development in the stressed plants. However, transcriptomic and chromatin analyses were carried out on immature leaves and no differences in vegetative development (i.e. number of leaves, growth stage of sampled leaves) were observed in stressed plants. Since it is well known that leaf-derived floral molecular signals regulate flowering in maize (Dong *et al.* 2012), it could be speculated that their drought-induced mis-regulation alters inflorescence development. By investigating drought stress induced changes in maize small RNA accumulation (Lunardon, Forestan, Farinati, Axtell & Varotto 2016), we observed the upregulation of miR156, which is involved in floral transition in *Arabidopsis* as negative

regulator of SQUAMOSA PROMOTER BINDING PROTEIN LIKE (SPL; Wu and Poethig, 2006). In maize, miRNA156 negatively regulates the expression of *TSH4*, *UB2*, and *UB3* (Chuck, Meeley, Irish, Sakai & Hake 2007; Chuck, Whipple, Jackson & Hake 2010; Chuck, Brown, Meeley & Hake 2014; Wei, Zhao, Xie & Wang 2018), three SPL floral regulators which expression is altered after drought stress. Moreover, SPL gene family has recently been reported to function as a molecular link between drought stress signaling and developmental signaling in maize (Mao *et al.* 2016; Miao *et al.* 2017).

Concluding, by integrating transcriptome and chromatin omics we provided data to evaluate how maize plants modulate their response to a mild water stress, adapt to it and do recover from the stress. The identification of transcriptional memory targets, their associated dynamic chromatin mark changes and putative memory marks suggests that mechanisms underlying the stress memory behavior will most likely function in a gene- (or subset-) specific manner. Stress-responsive genes in which variations of transcript levels persist after recovery (i.e. *ZEP1*, *NCED6*, and members of AP2/EREBP, NAC and WRKY TFs families), as well as genes not showing an immediate response to stress, but perceiving and storing stress signal for a delayed response (i.e. *MADS4* and *MADS15*) were identified. However, according to the accepted definition, a memory (epigenetic) mark persist longer, after the transcription is no longer active, and should affect the genes' transcriptional performances in subsequent stresses (Ding *et al.* 2012; Liu *et al.* 2014b; Avramova 2015). In this operational definition, the stable or delayed stress-induced chromatin mark changes observed in ST Stable and SR clusters and not directly associated to transcription activity may represent putative memory marks, although their impact on transcriptional regulation during subsequent stresses should be further investigated.

Acknowledgments

The work was financially supported by special grants from the European Commission (FP7 Project KBBE 2009 226477 - “AENEAS”: Acquired Environmental Epigenetics Advances: from Arabidopsis to maize), Italian CNR Flagship project EPIGEN the COST Action Impact of Nuclear Domains on Gene Expression and Plant Traits (INDEPTH, CA16212).

The authors would like to thank Prof. Zoya Avramova, Prof Hank Bass, Prof. Fiorella Lo Schiavo, Dr. Massimiliano Lauria and Dr. Nicola Carraro for critical reading of the manuscript and helpful comments, and Prof. Benedetto Ruperti for use of the microscope.

Data availability

RNA-Seq and ChIP-Seq data from this article can be found in the Gene Expression Omnibus data library under accession number accession number GSE71046

(<https://www.ncbi.nlm.nih.gov/geo/query/acc.cgi?acc=GSE71046>) and GSE128002

(<https://www.ncbi.nlm.nih.gov/geo/query/acc.cgi?acc=GSE128002>), respectively.

References

- Alter P., Bircheneder S., Zhou L.-Z., Schlüter U., Gahrtz M., Sonnewald U. & Dresselhaus T. (2016) Flowering Time-Regulated Genes in Maize Include the Transcription Factor ZmMADS1. *Plant physiology* **172**, 389–404.
- Anders S., Pyl P.T. & Huber W. (2015) HTSeq--a Python framework to work with high-throughput sequencing data. *Bioinformatics* **31**, 166–169.
- Asensi-Fabado M.A., Amtmann A. & Perrella G. (2017) Plant responses to abiotic stress: The chromatin context of transcriptional regulation. *Biochimica et biophysica acta* **1860**, 106–122.
- Avramova V., Abdelgawad H., Zhang Z., Fotschki B., Casadevall R., Vergauwen L., ... Beemster G.T.S. (2015) Drought Induces Distinct Growth Response, Protection, and

- Recovery Mechanisms in the Maize Leaf Growth Zone. *Plant Physiology* **169**, 1382–1396.
- Avramova Z. (2015) Transcriptional ‘memory’ of a stress: transient chromatin and memory (epigenetic) marks at stress-response genes. *The Plant Journal* **83**, 149–159.
- Bänziger M. & Araus J.-L. (2007) Recent Advances in Breeding Maize for Drought and Salinity Stress Tolerance. In *Advances in Molecular Breeding Toward Drought and Salt Tolerant Crops*. pp. 587–601. Springer Netherlands, Dordrecht.
- Bäurle I. (2018) Can’t remember to forget you: Chromatin-based priming of somatic stress responses. *Seminars in cell & developmental biology* **83**, 133–139.
- Begcy K. & Dresselhaus T. (2018) Epigenetic responses to abiotic stresses during reproductive development in cereals. *Plant Reproduction* **31**, 343–355.
- BENDIX C., MENDOZA J.M., STANLEY D.N., MEELEY R. & HARMON F.G. (2013) The circadian clock-associated gene *gigantea1* affects maize developmental transitions. *Plant, Cell & Environment* **36**, 1379–1390.
- Blum A. (2014) *Genomics for drought resistance - getting down to earth*.
- Charron J.-B.F., He H., Elling A.A. & Deng X.W. (2009) Dynamic landscapes of four histone modifications during deetiolation in Arabidopsis. *The Plant cell* **21**, 3732–48.
- Chatterjee M., Tabi Z., Galli M., Malcomber S., Buck A., Muszynski M. & Gallavotti A. (2014) The Boron Efflux Transporter ROTTEN EAR Is Required for Maize Inflorescence Development and Fertility. *The Plant Cell* **26**, 2962–2977.
- Chaves M.M., Flexas J. & Pinheiro C. (2009) Photosynthesis under drought and salt stress: regulation mechanisms from whole plant to cell. *Annals of botany* **103**, 551–60.
- Chen W.J. & Zhu T. (2004) Networks of transcription factors with roles in environmental stress response. *Trends in plant science* **9**, 591–596.
- Chinnusamy V. & Zhu J.-K. (2009) Epigenetic regulation of stress responses in plants. *Current Opinion in Plant Biology* **12**, 133–139.
- Chuck G., Meeley R., Irish E., Sakai H. & Hake S. (2007) The maize tasselseed4 microRNA controls sex determination and meristem cell fate by targeting

Tasselseed6/indeterminate spikelet1. *Nature Genetics* **39**, 1517–1521.

Chuck G., Whipple C., Jackson D. & Hake S. (2010) The maize SBP-box transcription factor encoded by tasselsheath4 regulates bract development and the establishment of meristem boundaries. *Development* **137**, 1243–1250.

Chuck G.S., Brown P.J., Meeley R. & Hake S. (2014) Maize SBP-box transcription factors unbranched2 and unbranched3 affect yield traits by regulating the rate of lateral primordia initiation. *Proceedings of the National Academy of Sciences* **111**, 18775–18780.

Colasanti J., Yuan Z. & Sundaresan V. (1998) The indeterminate gene encodes a zinc finger protein and regulates a leaf-generated signal required for the transition to flowering in maize. *Cell* **93**, 593–603.

Conesa A. & Gotz S. (2008) Blast2GO: A comprehensive suite for functional analysis in plant genomics. *International journal of plant genomics* **2008**, 619832.

Cook B.I., Anchukaitis K.J., Touchan R., Meko D.M. & Cook E.R. (2016) Spatiotemporal drought variability in the Mediterranean over the last 900 years. *Journal of Geophysical Research: Atmospheres* **121**, 2060–2074.

Crisp P.A., Ganguly D., Eichten S.R., Borevitz J.O. & Pogson B.J. (2016) Reconsidering plant memory: Intersections between stress recovery, RNA turnover, and epigenetics. *Science Advances* **2**, e1501340.

Danilevskaya O.N., Meng X., Selinger D.A., Deschamps S., Hermon P., Vansant G., ... Muszynski M.G. (2008) Involvement of the MADS-box gene ZMM4 in floral induction and inflorescence development in maize. *Plant Physiology* **147**, 2054–2069.

van Dijk K., Ding Y., Malkaram S., Riethoven J.-J.M., Liu R., Yang J., ... Fromm M. (2010) Dynamic Changes in Genome-Wide Histone H3 Lysine 4 Methylation Patterns in Response to Dehydration Stress in *Arabidopsis thaliana*. *BMC Plant Biology* **10**, 238.

Ding Y., Fromm M. & Avramova Z. (2012) Multiple exposures to drought “train” transcriptional responses in *Arabidopsis*. *Nature Communications* **3**, 740.

Ding Y., Liu N., Virilouvet L., Riethoven J.-J., Fromm M. & Avramova Z. (2013) Four distinct types of dehydration stress memory genes in *Arabidopsis thaliana*. *BMC plant*

biology **13**, 229.

- Ding Y., Virilouvet L., Liu N., Riethoven J.-J., Fromm M. & Avramova Z. (2014) Dehydration stress memory genes of *Zea mays*; comparison with *Arabidopsis thaliana*. *BMC plant biology* **14**, 141.
- Dong Z., Danilevskaya O., Abadie T., Messina C., Coles N. & Cooper M. (2012) A Gene Regulatory Network Model for Floral Transition of the Shoot Apex in Maize and Its Dynamic Modeling. *PLoS ONE* **7**, e43450.
- Du Z., Li H., Wei Q., Zhao X., Wang C., Zhu Q., ... Su Z. (2013) Genome-Wide Analysis of Histone Modifications: H3K4me2, H3K4me3, H3K9ac, and H3K27ac in *Oryza sativa* L. Japonica. *Molecular Plant* **6**, 1463–1472.
- Engelhorn J., Blanvillain R., Kröner C., Parrinello H., Rohmer M., Posé D., ... Carles C.C. (2017) Dynamics of H3K4me3 Chromatin Marks Prevails over H3K27me3 for Gene Regulation during Flower Morphogenesis in *Arabidopsis thaliana*. *Epigenomes* **1**, 8.
- Fabbro C. Del, Scalabrin S., Morgante M. & Giorgi F.M. (2013) An extensive evaluation of read trimming effects on Illumina NGS data analysis. *PloS one* **8**, e85024.
- Feng X.J., Li J.R., Qi S.L., Lin Q.F., Jin J.B. & Hua X.J. (2016) Light affects salt stress-induced transcriptional memory of *P5CS1* in *Arabidopsis*. *Proceedings of the National Academy of Sciences* **113**, E8335–E8343.
- Forestan C., Aiese Cigliano R., Farinati S., Lunardon A., Sanseverino W. & Varotto S. (2016) Stress-induced and epigenetic-mediated maize transcriptome regulation study by means of transcriptome reannotation and differential expression analysis. *Scientific Reports* **6**.
- Forestan C., Farinati S., Aiese Cigliano R., Lunardon A., Sanseverino W. & Varotto S. (2017) Maize RNA PolIV affects the expression of genes with nearby TE insertions and has a genome-wide repressive impact on transcription. *BMC Plant Biology* **17**.
- Forestan C., Farinati S., Rouster J., Lassagne H., Lauria M., Dal Ferro N. & Varotto S. (2018) Control of maize vegetative and reproductive development, fertility, and rRNAs silencing by histone deacetylase 108. *Genetics* **208**.
- Friedrich T., Faivre L., Bäurle I. & Schubert D. (2018) Chromatin-based mechanisms of

temperature memory in plants. *Plant, cell & environment*.

Galbiati F., Chiozzotto R., Locatelli F., Spada A., Genga A. & Fornara F. (2016) Hd3a, RFT1 and Ehd1 integrate photoperiodic and drought stress signals to delay the floral transition in rice. *Plant, Cell & Environment* **39**, 1982–1993.

Granier C., Inzé D. & Tardieu F. (2000) Spatial distribution of cell division rate can be deduced from that of p34(cdc2) kinase activity in maize leaves grown at contrasting temperatures and soil water conditions. *Plant physiology* **124**, 1393–402.

Haak D.C., Fukao T., Grene R., Hua Z., Ivanov R., Perrella G. & Li S. (2017) Multilevel Regulation of Abiotic Stress Responses in Plants. *Frontiers in plant science* **8**, 1564.

He G., Chen B., Wang X., Li X., Li J., He H., ... Wang Deng X. (2013) Conservation and divergence of transcriptomic and epigenomic variation in maize hybrids. *Genome Biology* **14**, R57.

He G., Zhu X., Elling A.A., Chen L., Wang X., Guo L., ... Deng X.-W. (2010) Global epigenetic and transcriptional trends among two rice subspecies and their reciprocal hybrids. *The Plant cell* **22**, 17–33.

Hempel F.D., Welch D.R. & Feldman L.J. (2000) Floral induction and determination: where is flowering controlled? *Trends in Plant Science* **5**, 17–21.

Hu Y., Liu D., Zhong X., Zhang C., Zhang Q. & Zhou D.-X. (2012a) CHD3 protein recognizes and regulates methylated histone H3 lysines 4 and 27 over a subset of targets in the rice genome. *Proceedings of the National Academy of Sciences of the United States of America* **109**, 5773–8.

Hu Y., Zhang L., He S., Huang M., Tan J., Zhao L., ... Li L. (2012b) Cold stress selectively unsilences tandem repeats in heterochromatin associated with accumulation of H3K9ac. *Plant, Cell & Environment* **35**, 2130–2142.

Huan Q., Mao Z., Chong K. & Zhang J. (2018) Global analysis of H3K4me3/H3K27me3 in *Brachypodium distachyon* reveals VRN3 as critical epigenetic regulation point in vernalization and provides insights into epigenetic memory. *New Phytologist* **219**, 1373–1387.

Hyun Y., Richter R. & Coupland G. (2017) Competence to Flower: Age-Controlled

Sensitivity to Environmental Cues. *Plant Physiology* **173**, 36–46.

Iuchi S., Kobayashi M., Taji T., Naramoto M., Seki M., Kato T., ... Shinozaki K. (2001) Regulation of drought tolerance by gene manipulation of 9-cis-epoxycarotenoid dioxygenase, a key enzyme in abscisic acid biosynthesis in *Arabidopsis*. *The Plant Journal* **27**, 325–33.

Janiak A., Kwaśniewski M. & Szarejko I. (2016) Gene expression regulation in roots under drought. *Journal of Experimental Botany* **67**, 1003–1014.

Jia J., Fu J., Zheng J., Zhou X., Huai J., Wang J., ... Wang G. (2006) Annotation and expression profile analysis of 2073 full-length cDNAs from stress-induced maize (*Zea mays* L.) seedlings. *The Plant Journal* **48**, 710–727.

Jiao Y., Peluso P., Shi J., Liang T., Stitzer M.C., Wang B., ... Ware D. (2017) Improved maize reference genome with single-molecule technologies. *Nature* **546**, 524–527.

Jin M., Liu X., Jia W., Liu H., Li W., Peng Y., ... Yan J. (2018) ZmCOL3, a CCT gene represses flowering in maize by interfering with the circadian clock and activating expression of ZmCCT. *Journal of integrative plant biology* **60**, 465–480.

Joshi R., Wani S.H., Singh B., Bohra A., Dar Z.A., Lone A.A., ... Singla-Pareek S.L. (2016) Transcription Factors and Plants Response to Drought Stress: Current Understanding and Future Directions. *Frontiers in plant science* **7**, 1029.

Kazan K. & Lyons R. (2016) The link between flowering time and stress tolerance. *Journal of Experimental Botany* **67**, 47–60.

Kim D., Pertea G., Trapnell C., Pimentel H., Kelley R. & Salzberg S.L. (2013) TopHat2: accurate alignment of transcriptomes in the presence of insertions, deletions and gene fusions. *Genome biology* **14**, R36-2013-14-4-r36.

Kim J.-M., To T.K., Ishida J., Matsui A., Kimura H. & Seki M. (2012) Transition of Chromatin Status During the Process of Recovery from Drought Stress in *Arabidopsis thaliana*. *Plant and Cell Physiology* **53**, 847–856.

Kim J.-M., To T.K., Ishida J., Morosawa T., Kawashima M., Matsui A., ... Seki M. (2008) Alterations of Lysine Modifications on the Histone H3 N-Tail under Drought Stress Conditions in *Arabidopsis thaliana*. *Plant and Cell Physiology* **49**, 1580–1588.

Kwon C.S., Lee D., Choi G. & Chung W.-I. (2009) Histone occupancy-dependent and -independent removal of H3K27 trimethylation at cold-responsive genes in Arabidopsis. *The Plant journal : for cell and molecular biology* **60**, 112–21.

Lafos M., Kroll P., Hohenstatt M.L., Thorpe F.L., Clarenz O. & Schubert D. (2011) Dynamic Regulation of H3K27 Trimethylation during Arabidopsis Differentiation. *PLoS Genetics* **7**, e1002040.

Lamke J. & Baurle I. (2017) Epigenetic and chromatin-based mechanisms in environmental stress adaptation and stress memory in plants. *Genome biology* **18**, 124-017-1263–6.

Lamke J., Brzezinka K., Altmann S. & Baurle I. (2016) A hit-and-run heat shock factor governs sustained histone methylation and transcriptional stress memory. *The EMBO Journal* **35**, 162–175.

Langmead B. & Salzberg S.L. (2012) Fast gapped-read alignment with Bowtie 2. *Nature methods* **9**, 357–9.

Lawit S.J., Wych H.M., Xu D., Kundu S. & Tomes D.T. (2010) Maize DELLA Proteins dwarf plant8 and dwarf plant9 as Modulators of Plant Development. *Plant and Cell Physiology* **51**, 1854–1868.

Lazakis C.M., Coneva V. & Colasanti J. (2011) ZCN8 encodes a potential orthologue of Arabidopsis FT florigen that integrates both endogenous and photoperiod flowering signals in maize. *Journal of Experimental Botany* **62**, 4833–4842.

Li S., Lin Y.-C.J., Wang P., Zhang B., Li M., Chen S., ... Li W. (2018) Histone Acetylation Cooperating with AREB1 Transcription Factor Regulates Drought Response and Tolerance in Populus trichocarpa. *The Plant Cell*, tpc.00437.2018.

Li T., Chen X., Zhong X., Zhao Y., Liu X., Zhou S., ... Zhou D.-X. (2013) Jumonji C Domain Protein JMJ705-Mediated Removal of Histone H3 Lysine 27 Trimethylation Is Involved in Defense-Related Gene Activation in Rice. *The Plant Cell* **25**, 4725–4736.

Liu L., Wu Y., Liao Z., Xiong J., Wu F., Xu J., ... Lu Y. (2018) Evolutionary conservation and functional divergence of the LFK gene family play important roles in the photoperiodic flowering pathway of land plants. *Heredity* **120**, 310–328.

Liu N., Ding Y., Fromm M. & Avramova Z. (2014a) Different gene-specific mechanisms

- determine the 'revised-response' memory transcription patterns of a subset of *A. thaliana* dehydration stress responding genes. *Nucleic Acids Research* **42**, 5556–5566.
- Liu N., Fromm M. & Avramova Z. (2014b) H3K27me3 and H3K4me3 Chromatin Environment at Super-Induced Dehydration Stress Memory Genes of *Arabidopsis thaliana*. *Molecular Plant* **7**, 502–513.
- Liu X., Zhou S., Wang W., Ye Y., Zhao Y., Xu Q., ... Zhou D.-X. (2015) Regulation of histone methylation and reprogramming of gene expression in the rice inflorescence meristem. *The Plant cell* **27**, 1428–44.
- Lu H.F., Dong H.T., Sun C.B., Qing D.J., Li N., Wu Z.K., ... Li Y.Z. (2011) The panorama of physiological responses and gene expression of whole plant of maize inbred line YQ7-96 at the three-leaf stage under water deficit and re-watering. *TAG. Theoretical and applied genetics. Theoretische und angewandte Genetik* **123**, 943–958.
- Lunardon A., Forestan C., Farinati S., Axtell M.J. & Varotto S. (2016) Genome-wide characterization of maize small RNA loci and their regulation in the Required to maintain repression6-1 (Rmr6-1) mutant and long-term abiotic stresses. *Plant Physiology* **170**.
- Mao H.-D., Yu L.-J., Li Z.-J., Yan Y., Han R., Liu H. & Ma M. (2016) Genome-wide analysis of the SPL family transcription factors and their responses to abiotic stresses in maize. *Plant Gene* **6**, 1–12.
- Martin M. (2011) Cutadapt removes adapter sequences from high-throughput sequencing reads. *EMBnet.journal* **17**, 10–12.
- Meng X., Muszynski M.G. & Danilevskaya O.N. (2011) The FT-Like ZCN8 Gene Functions as a Floral Activator and Is Involved in Photoperiod Sensitivity in Maize. *The Plant Cell* **23**, 942–960.
- Miao Z., Han Z., Zhang T., Chen S. & Ma C. (2017) A systems approach to a spatio-temporal understanding of the drought stress response in maize. *Scientific reports* **7**, 6590–017–06929–y.
- Miller T.A., Muslin E.H. & Dorweiler J.E. (2008) A maize CONSTANS-like gene, *conz1*, exhibits distinct diurnal expression patterns in varied photoperiods. *Planta* **227**, 1377–

- Minow M.A.A., Ávila L.M., Turner K., Ponzoni E., Mascheretti I., Dussault F.M., ... Colasanti J. (2018) Distinct gene networks modulate floral induction of autonomous maize and photoperiod-dependent teosinte. *Journal of experimental botany* **69**, 2937–2952.
- Mishra P. & Panigrahi K.C. (2015) GIGANTEA - an emerging story. *Frontiers in Plant Science* **6**, 8.
- Morari F., Meggio F., Lunardon A., Scudiero E., Forestan C., Farinati S. & Varotto S. (2015) Time course of biochemical, physiological, and molecular responses to field-mimicked conditions of drought, salinity, and recovery in two maize lines. *Frontiers in Plant Science* **6**.
- Muszynski M.G., Dam T., Li B., Shirbroun D.M., Hou Z., Bruggemann E., ... Danilevskaya O.N. (2006) delayed flowering1 Encodes a Basic Leucine Zipper Protein That Mediates Floral Inductive Signals at the Shoot Apex in Maize. *PLANT PHYSIOLOGY* **142**, 1523–1536.
- Nakashima K., Yamaguchi-Shinozaki K. & Shinozaki K. (2014) The transcriptional regulatory network in the drought response and its crosstalk in abiotic stress responses including drought, cold, and heat. *Frontiers in plant science* **5**, 170.
- Opitz N., Paschold A., Marcon C., Malik W.A., Lanz C., Piepho H.P. & Hochholdinger F. (2014) Transcriptomic complexity in young maize primary roots in response to low water potentials. *BMC genomics* **15**, 741-2164-15-741.
- Pfaffl M.W. (2001) A new mathematical model for relative quantification in real-time RT-PCR. *Nucleic acids research* **29**, e45.
- Qian S., Lv X., Scheid R.N., Lu L., Yang Z., Chen W., ... Du J. (2018) Dual recognition of H3K4me3 and H3K27me3 by a plant histone reader SHL. *Nature Communications* **9**, 2425.
- R Core Team (2017) R: A Language and Environment for Statistical Computing.
- Ramírez F., Ryan D.P., Grüning B., Bhardwaj V., Kilpert F., Richter A.S., ... Manke T. (2016) deepTools2: a next generation web server for deep-sequencing data analysis.

Nucleic Acids Research **44**, W160–W165.

Sani E., Herzyk P., Perrella G., Colot V. & Amtmann A. (2013) Hyperosmotic priming of Arabidopsis seedlings establishes a long-term somatic memory accompanied by specific changes of the epigenome. *Genome Biology* **14**, R59.

Seager R., Tzanova A. & Nakamura J. (2009) Drought in the Southeastern United States: Causes, Variability over the Last Millennium, and the Potential for Future Hydroclimate Change. *Journal of Climate* **22**, 5021–5045.

Seo M. & Koshiba T. (2002) Complex regulation of ABA biosynthesis in plants. *Trends in plant science* **7**, 41–8.

Shan X., Li Y., Jiang Y., Jiang Z., Hao W. & Yuan Y. (2013) Transcriptome Profile Analysis of Maize Seedlings in Response to High-salinity, Drought and Cold Stresses by Deep Sequencing. *Plant Molecular Biology Reporter* **31**, 1485–1491.

Song J., Guo B., Song F., Peng H., Yao Y., Zhang Y., ... Ni Z. (2011) Genome-wide identification of gibberellins metabolic enzyme genes and expression profiling analysis during seed germination in maize. *Gene* **482**, 34–42.

Song N., Xu Z., Wang J., Qin Q., Jiang H., Si W. & Li X. (2018) Genome-wide analysis of maize CONSTANS-LIKE gene family and expression profiling under light/dark and abscisic acid treatment. *Gene* **673**, 1–11.

Song Y.H., Ito S. & Imaizumi T. (2013) Flowering time regulation: photoperiod- and temperature-sensing in leaves. *Trends in plant science* **18**, 575–83.

Song Z.-T., Sun L., Lu S.-J., Tian Y., Ding Y. & Liu J.-X. (2015) Transcription factor interaction with COMPASS-like complex regulates histone H3K4 trimethylation for specific gene expression in plants. *Proceedings of the National Academy of Sciences* **112**, 2900–2905.

Takeno K. (2016) Stress-induced flowering: the third category of flowering response. *Journal of Experimental Botany* **67**, 4925–4934.

Tan B.-C., Joseph L.M., Deng W.-T., Liu L., Li Q.-B., Cline K. & McCarty D.R. (2003) Molecular characterization of the Arabidopsis 9-cis epoxy-carotenoid dioxygenase gene family. *The Plant Journal* **35**, 44–56.

- Tan B.C., Schwartz S.H., Zeevaart J.A. & McCarty D.R. (1997) Genetic control of abscisic acid biosynthesis in maize. *Proceedings of the National Academy of Sciences of the United States of America* **94**, 12235–40.
- Tenaillon M.I., Seddiki K., Mollion M., Guilloux M. Le, Marchadier E., Ressayre A. & Dillmann C. (2018) Transcriptomic response to divergent selection for flowering time in maize reveals convergence and key players of the underlying gene regulatory network. *bioRxiv*, 461947.
- Thimm O., Blasing O., Gibon Y., Nagel A., Meyer S., Kruger P., ... Stitt M. (2004) MAPMAN: a user-driven tool to display genomics data sets onto diagrams of metabolic pathways and other biological processes. *The Plant Journal* **37**, 914–939.
- Thornsberry J.M., Goodman M.M., Doebley J., Kresovich S., Nielsen D. & Buckler E.S. (2001) Dwarf8 polymorphisms associate with variation in flowering time. *Nature genetics* **28**, 286–9.
- Tiwari S., Lata C., Chauhan P.S., Prasad V. & Prasad M. (2017) A Functional Genomic Perspective on Drought Signalling and its Crosstalk with Phytohormone-mediated Signalling Pathways in Plants. *Current Genomics* **18**, 469–482.
- Trapnell C., Hendrickson D.G., Sauvageau M., Goff L., Rinn J.L. & Pachter L. (2013) Differential analysis of gene regulation at transcript resolution with RNA-seq. *Nature biotechnology* **31**, 46–53.
- Turck F., Roudier F., Farrona S., Martin-Magniette M.-L., Guillaume E., Buisine N., ... Colot V. (2007) Arabidopsis TFL2/LHP1 Specifically Associates with Genes Marked by Trimethylation of Histone H3 Lysine 27. *PLoS Genetics* **3**, e86.
- Tuteja N. (2007) Abscisic Acid and abiotic stress signaling. *Plant signaling & behavior* **2**, 135–8.
- Usadel B., Poree F., Nagel A., Lohse M., Czedik-Eysenberg A. & Stitt M. (2009) A guide to using MapMan to visualize and compare Omics data in plants: a case study in the crop species, Maize. *Plant, Cell & Environment* **32**, 1211–1229.
- Vergara Z. & Gutierrez C. (2017) Emerging roles of chromatin in the maintenance of genome organization and function in plants. *Genome Biology* **18**, 96.

- Virloquet L., Avenson T.J., Du Q., Zhang C., Liu N., Fromm M., ... Russo S.E. (2018) Dehydration Stress Memory: Gene Networks Linked to Physiological Responses During Repeated Stresses of *Zea mays*. *Frontiers in Plant Science* **9**, 1058.
- Voigt P., Tee W.-W. & Reinberg D. (2013) A double take on bivalent promoters. *Genes & development* **27**, 1318–38.
- Wang H. & Wang H. (2015) The miR156/SPL Module, a Regulatory Hub and Versatile Toolbox, Gears up Crops for Enhanced Agronomic Traits. *Molecular Plant* **8**, 677–688.
- Wang X., Elling A.A., Li X., Li N., Peng Z., He G., ... Deng X.W. (2009) Genome-wide and organ-specific landscapes of epigenetic modifications and their relationships to mRNA and small RNA transcriptomes in maize. *The Plant Cell* **21**, 1053–1069.
- Wei H., Zhao Y., Xie Y. & Wang H. (2018) Exploiting SPL genes to improve maize plant architecture tailored for high-density planting. *Journal of Experimental Botany* **69**, 4675–4688.
- Wickham H. (2009) *ggplot2: Elegant Graphics for Data Analysis*. Springer-Verlag New York.
- Wimalanathan K., Friedberg I., Andorf C.M. & Lawrence-Dill C.J. (2018) Maize GO Annotation-Methods, Evaluation, and Review (maize-GAMER). *Plant Direct* **2**, e00052.
- Wong A.Y.M. & Colasanti J. (2006) Maize floral regulator protein INDETERMINATE1 is localized to developing leaves and is not altered by light or the sink/source transition. *Journal of Experimental Botany* **58**, 403–414.
- Wu G. & Poethig R.S. (2006) Temporal regulation of shoot development in *Arabidopsis thaliana* by miR156 and its target SPL3. *Development (Cambridge, England)* **133**, 3539–3547.
- Wu S., Ning F., Zhang Q., Wu X. & Wang W. (2017) Enhancing Omics Research of Crop Responses to Drought under Field Conditions. *Frontiers in plant science* **8**, 174.
- You Y., Sawikowska A., Neumann M., Posé D., Capovilla G., Langenecker T., ... Schmid M. (2017) Temporal dynamics of gene expression and histone marks at the *Arabidopsis* shoot meristem during flowering. *Nature Communications* **8**, 15120.

Zhang X., Bernatavichute Y. V, Cokus S., Pellegrini M. & Jacobsen S.E. (2009) Genome-wide analysis of mono-, di- and trimethylation of histone H3 lysine 4 in *Arabidopsis thaliana*. *Genome Biology* **10**, R62.

Zhang X., Clarenz O., Cokus S., Bernatavichute Y. V, Pellegrini M., Goodrich J. & Jacobsen S.E. (2007) Whole-Genome Analysis of Histone H3 Lysine 27 Trimethylation in *Arabidopsis*. *PLoS Biology* **5**, e129.

Zhang X., Lei L., Lai J., Zhao H. & Song W. (2018) Effects of drought stress and water recovery on physiological responses and gene expression in maize seedlings. *BMC plant biology* **18**, 68.

Zheng J., Fu J., Gou M., Huai J., Liu Y., Jian M., ... Wang G. (2010) Genome-wide transcriptome analysis of two maize inbred lines under drought stress. *Plant Molecular Biology* **72**, 407–421.

Zheng Y., Ding Y., Sun X., Xie S., Wang D., Liu X., ... Zhou D.-X. (2016) Histone deacetylase HDA9 negatively regulates salt and drought stress responsiveness in *Arabidopsis*. *Journal of Experimental Botany* **67**, 1703–1713.

Zhu J.-K. (2016) Abiotic Stress Signaling and Responses in Plants. *Cell* **167**, 313–324.

Tables

Table 1: Number of differentially expressed genes (DEGs) and their overlap at different time points.

	NST0 > WST0	NST0 < WST0	WST0 > WST7	WST0 < WST7	WST7 > NST7	WST7 < NST7
NST0 > WST0	1,957					
NST0 < WST0	X	794				
WST0 > WST7	1	199	250			
WST0 < WST7	314	0	X	383		
WST7 > NST7	2	1	0	6	23	
WST7 < NST7	0	2	4	0	X	13

Number of DEGs found up- or down-regulated in each growth condition and time point. The grey box displays the number of DEGs (up- or down-regulated) in one comparison, while white fields indicate overlapping with other comparisons.

Table 2: Summary of differentially marked genes (DMGs) dynamics profile assignment.

	H3K4me3	H3K9ac	H3K27me3
ST Gain Transient	1,335 (27.3%)	132 (6.8%)	108 (12.3%)
ST Gain Stable	71 (1.5%)	40 (2.1%)	50 (5.7%)
ST Loss Transient	1,245 (25.5%)	82 (4.2%)	/
ST Loss Stable	350 (7.2%)	224 (11.6%)	/
SR Gain	375 (7.7%)	180 (9.3%)	476 (54.2%)
SR Loss	270 (5.5%)	114 (5.9%)	62 (7.0%)
Other profiles	1,236 (25.3%)	1,163 (60.1%)	183 (20.8%)
Total DMGs	4,882	1,935	879

Number of genes assigned to each enrichment profile (cluster) and total DMGs for each analyzed histone modification.

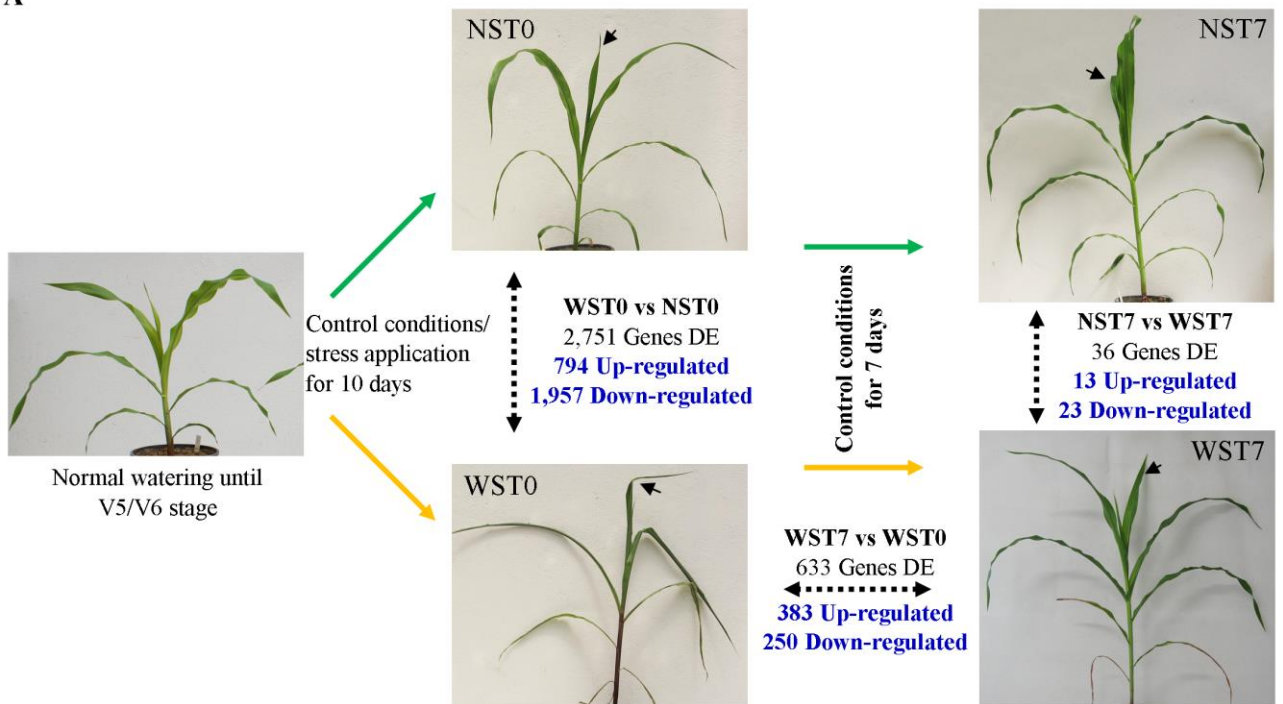
Accepted Article

Table 3: Details of drought-induced transcriptional and epigenomic changes at selected floral regulator genes.

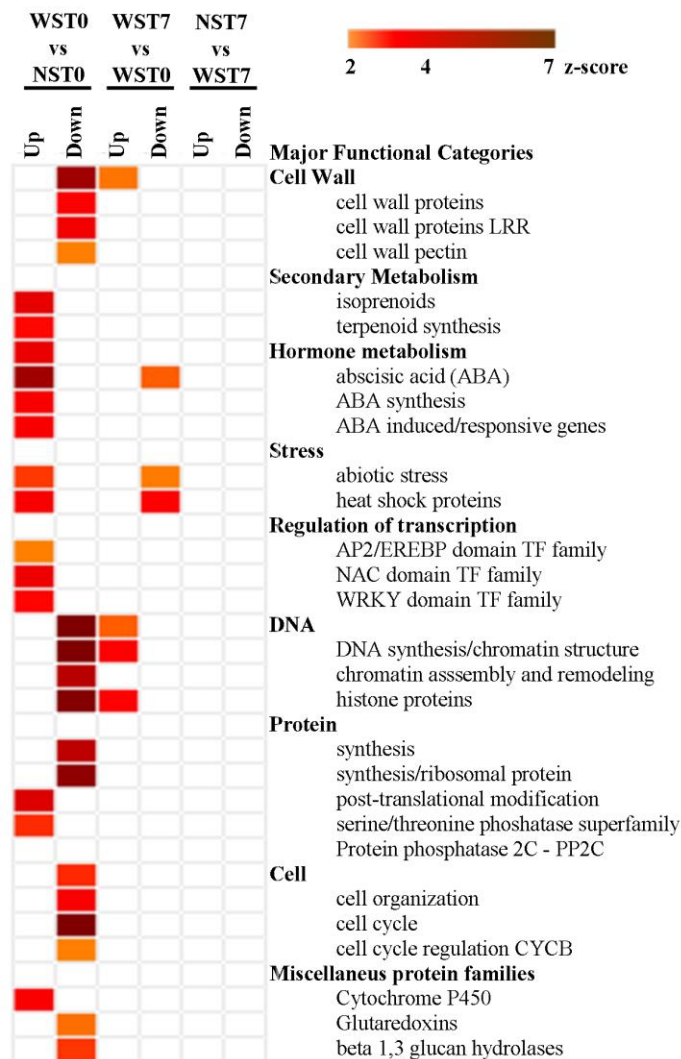
Gene ID and Symbol		log2FC (WST0/NST0)	log2FC (NST7/WST7)	DMGs Dynamic Cluster	References
Zm00001d032922	ID1	-1.15	-0.40†		Colasanti et al., 1998; Wong and Colasanti, 2006
Zm00001d010752	ZCN8	0.59†	0.44†		Lazakis et al., 2011; Meng et al., 2011
Zm00001d022613	DLF1	-1.15†	-0.08†		Muszynski et al., 2006
Zm00001d048474	MADS1	-0.09†	-0.03†		Alter et al., 2016
Zm00001d020941	TSH4	-1.28	0.10†	H3K4me3 ST Loss Trans.	Chuck et al., 2014, 2010;
Zm00001d031451	UB2	-1.83	0.17†		Wang and Wang, 2015;
Zm00001d052890	UB3	-1.07	0.23†		Wei et al., 2018
Zm00001d030656	RTE	-1.29	0.26†	H3K4me3 ST Loss Stable	Chatterjee et al., 2014
Zm00001d038695	GA2Ox7	-1.42	0.92†	H3K4me3 ST Gain Trans.	Song et al., 2011
Zm00001d033680	D8	-1.46	-0.02†		Thornsberry et al., 2001; Lawit et al., 2010
Zm00001d007445	FKF1	2.02	0.95†		Liu et al., 2018
Zm00001d053091	FKF2	2.05	1.35†	H3K4me3 SR Loss	
Zm00001d029149	COL15	1.09	0.07†		Song et al., 2018; Jin et al., 2018
Zm00001d008826	GI1	0.59†	0.01†		Miller et al., 2008;
Zm00001d039589	GI2	1.15	0.32†	H3K9ac ST Gain Trans.	Bendix et al., 2013
Zm00001d034045	MADS4	0.90†	2.08	H3K4me3 SR Loss; H3K27me3 ST Gain Trans.	Danilevskaya et al., 2008
Zm00001d013259	MADS15	-0.88†	2.12	H3K4me3 SR Loss; H3K27me3 SR Gain	

Pairwise differential expression results (reported as log2FC) and summary of chromatin profile cluster for each of the candidate floral regulators coding genes discussed in the main text. † = not significant expression changes

Figure 1
A



B Over-representation Analysis



C DEGs K-means clustering

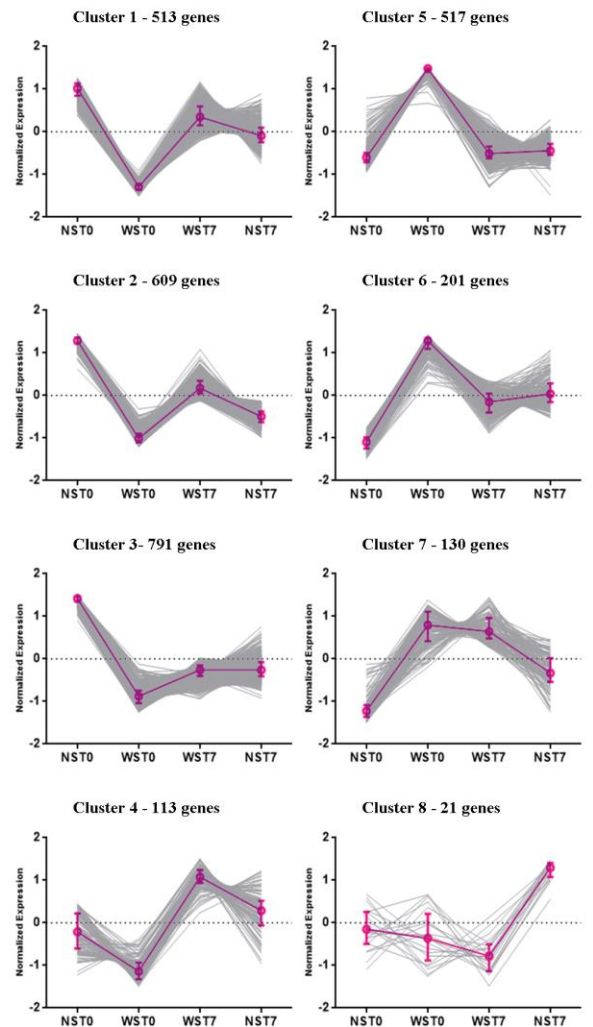


Figure 1. Experimental set-up and differential gene expression analysis results.

(A) Experimental design of drought stress application and post-stress recovery period. In each time-point, an arrow indicates the leaf sampled. The four samples NST0, WST0, WST7 and NST7 were analyzed by RNA-Seq and ChIP-Seq (H3K4me3, H3K27me3 and H3K9ac histone modifications). Numbers of differentially expressed genes (DEGs) in each pairwise comparison are reported. (B) MapMan functional categories enriched in the six DEG groups. Z-scores automatically calculated from p-values (e.g. 1.96 corresponds to a P-value of 0.05) are plotted in an orange to brown color scale. (C) Results of k-means clustering analysis with k=8, to generate an overview of DEGs expression profiles. The grey lines represent the single genes in the cluster; median and interquartile ranges of expression z-scores in each cluster are depicted in purple. NS = Not Stressed; WS = Water Stressed; T0 = end of stress application sampling time-point; T7: end of recovery sampling time-point.

Accepted Article

Figure 2

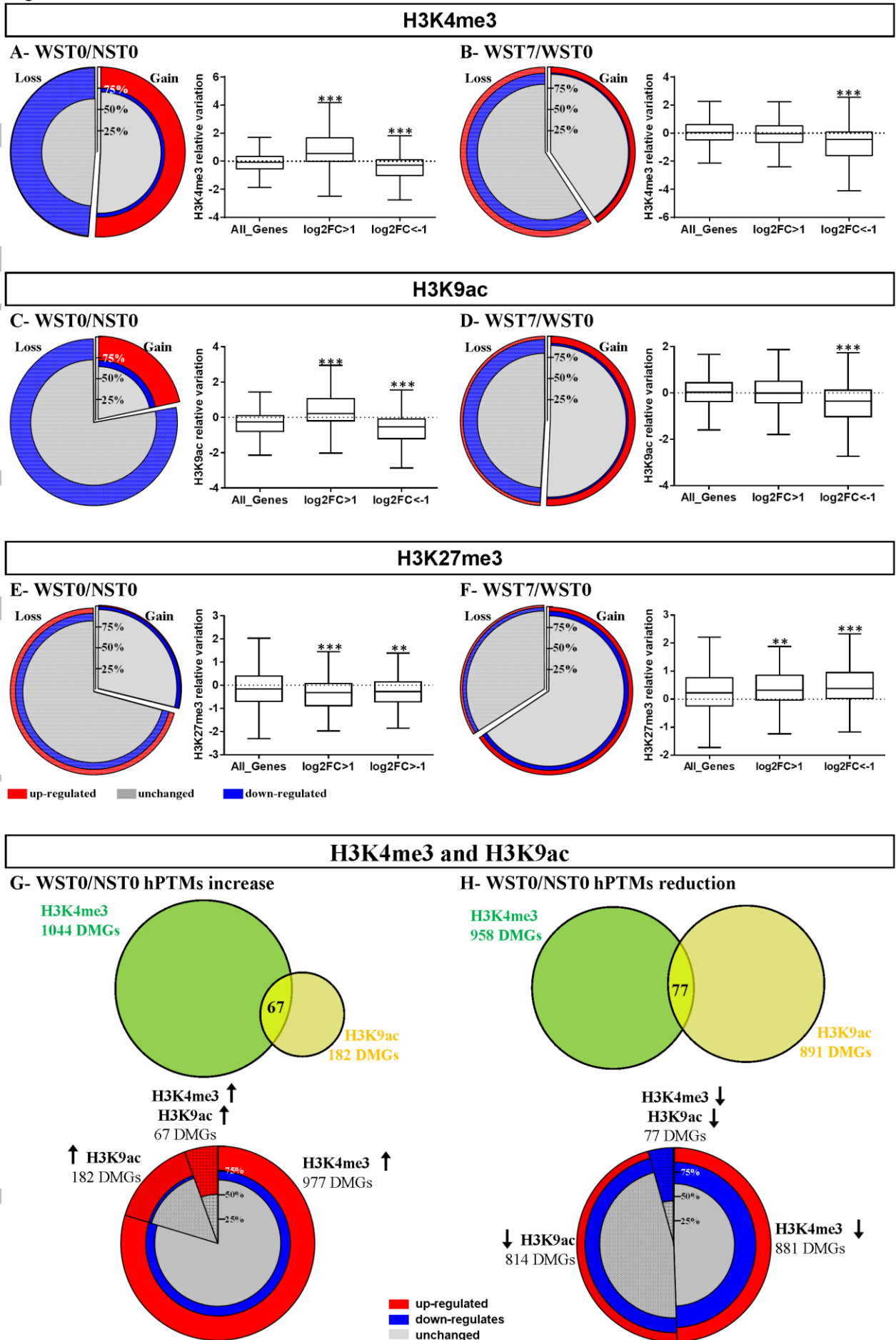


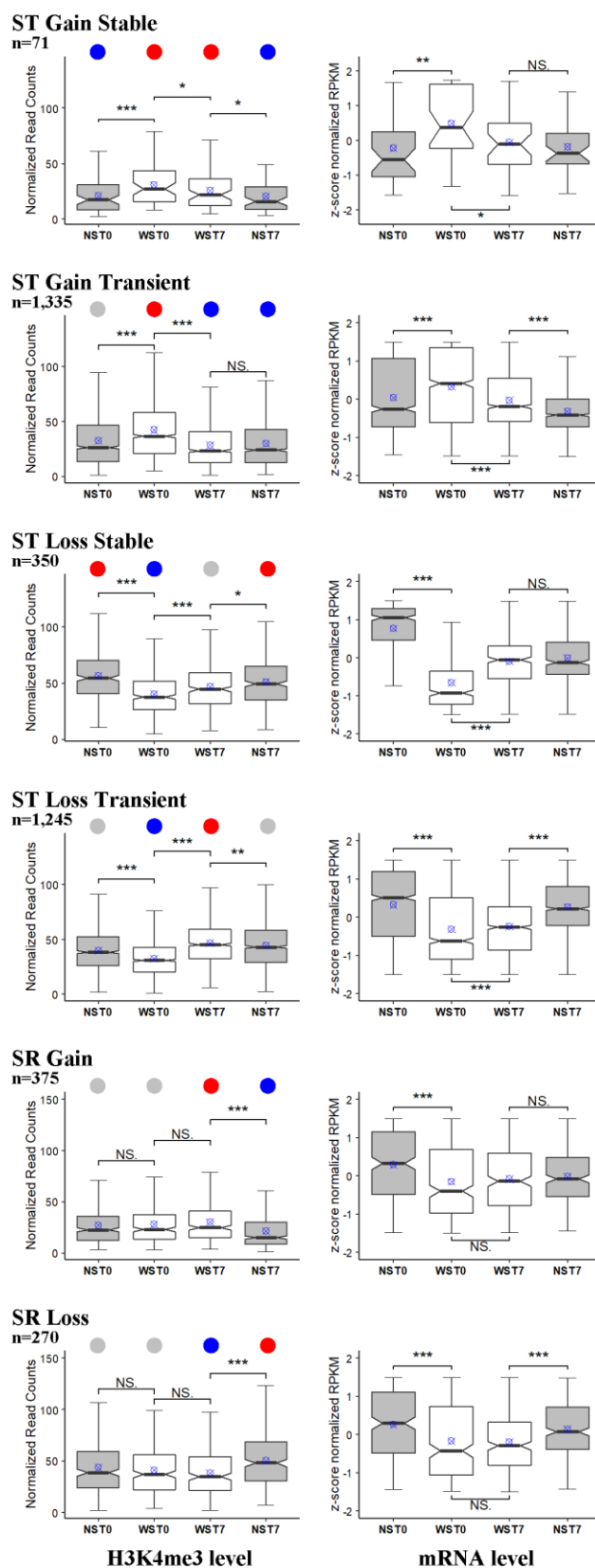
Figure 2. Correlation of changes in histone marks, expression changes after the stress application and recovery period and overlap between H3K4me3 and H3K9ac DMGs.

The correlation between histone changes and expression changes for H3K4me3 (A - B), H3K9ac (C - D), and H3K27me3 (E - F) for the WST0 vs NST0 (A, C and E) and WST7 vs WST0 (B, D and E) comparisons is reported as pie-charts and box-plots. In pie-charts, each piece of the pie depicts the proportion of DMGs showing significant increase or decrease of the histone mark and the pieces themselves are color-coded according to the number of differentially expressed genes (DEGs) in each group. Box-plots report the relative variation of histone mark levels at transcriptionally up- or down-regulated genes ($\log_2FC > 1$ and $\log_2FC < -1$, respectively), put alongside with the whole set of genes (being as both transcriptionally expressed and with histone mark enrichment compared to the whole chromatin).

For the WST0 vs NST0 pairwise comparison, the overlap between DMGs with concordant changes in H3K4me3 and H3K9ac and the impact of changes in only one or both marks on gene expression variations are reported as Venn diagrams and pie-charts (G - H). **: $p < 0.01$, ***: $p < 0.001$; Mann-Whitney U test.

Figure 3

H3K4me3 dynamic profiles



Legend:

- High level
- Medium level/ Mixed pattern
- Low level

Figure 3. Dynamic analysis of H3K4me3 reveals specific chromatin memory profiles that define transcriptional regulation in response to stress and recovery.

Hierarchical clustering of the 4,882 H3K4me3 differentially marked genes (DMGs) over the course of the experiment allowed the identification of 6 clusters with well-defined stress and recovery responsive dynamics (Figure S10). For genes within stress treatment (ST; stable or transient, gain and loss) and stress recovery clusters (SR; gain and loss), box plots on the left report H3K4me3 dynamics as normalized read counts, while RNA-Seq scaled expression levels (RPKM) of the genes in each clusters are plotted on the right (only expressed genes were included). These profiles comprise 3,646 (75%) DMGs. A schematic of chromatin variation patterns in the four analyzed samples is reported for each cluster. *: $p < 0.05$, **: $p < 0.01$, ***: $p < 0.001$, NS = not significant; Mann-Whitney U test.

Accepted Article

Figure 4

H3K9ac dynamic profiles

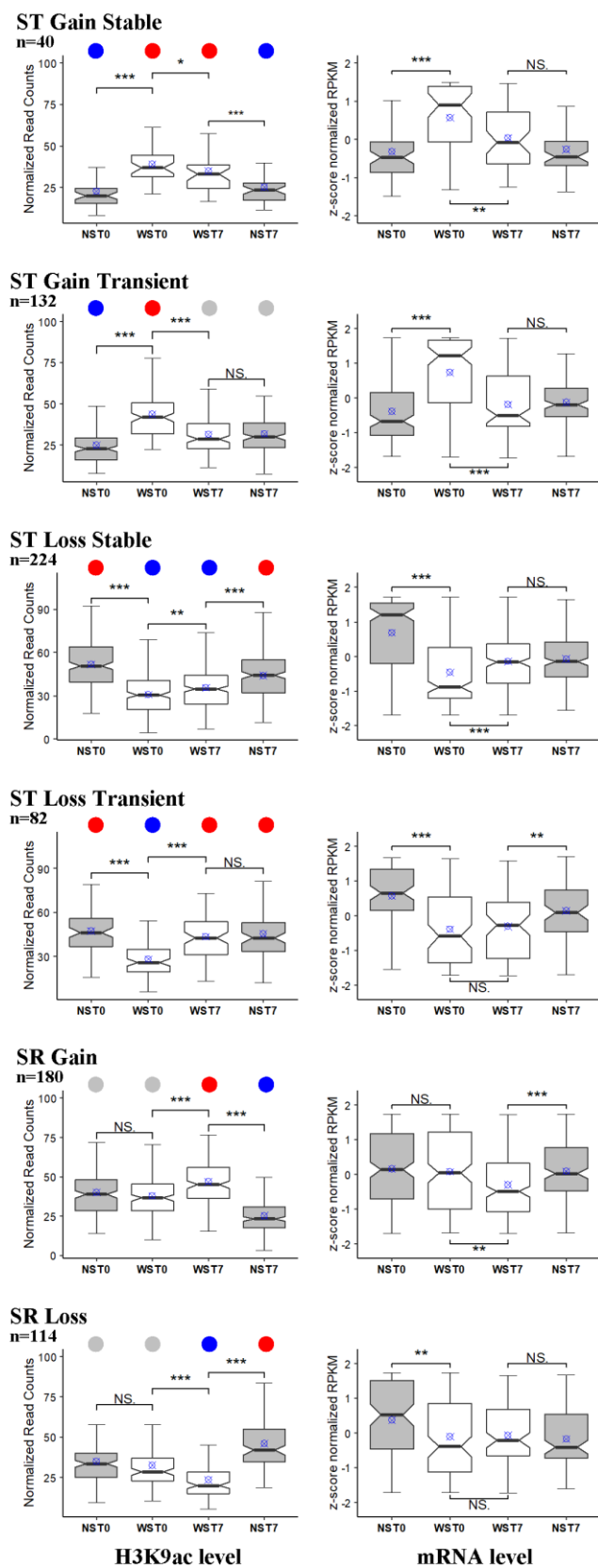


Figure 4. Dynamic analysis of H3K9ac reveals specific chromatin memory profiles that predict transcriptional regulation in response to stress but not after recovery.

Hierarchical clustering of the 1,935 H3K9ac differentially marked genes (DMGs) over the course of the experiment allowed the identification of 6 profiles with well-defined stress and recovery responsive dynamics (Figure S12). Stress treatment (ST; stable or transient, gain and loss) and stress recovery (SR; gain and loss) clusters include only a small fraction of DMGs (39.9%). For genes included in these groups, detailed H3K9ac dynamics are reported in left box-plots as normalized read counts, while RNA-Seq scaled expression levels (RPKM) of the expressed genes in each clusters are plotted to the right. A schematic of chromatin variation patterns in the four analyzed samples is reported for each cluster. *: $p < 0.05$, **: $p < 0.01$, ***: $p < 0.001$, NS = not significant; Mann-Whitney U test.

Accepted

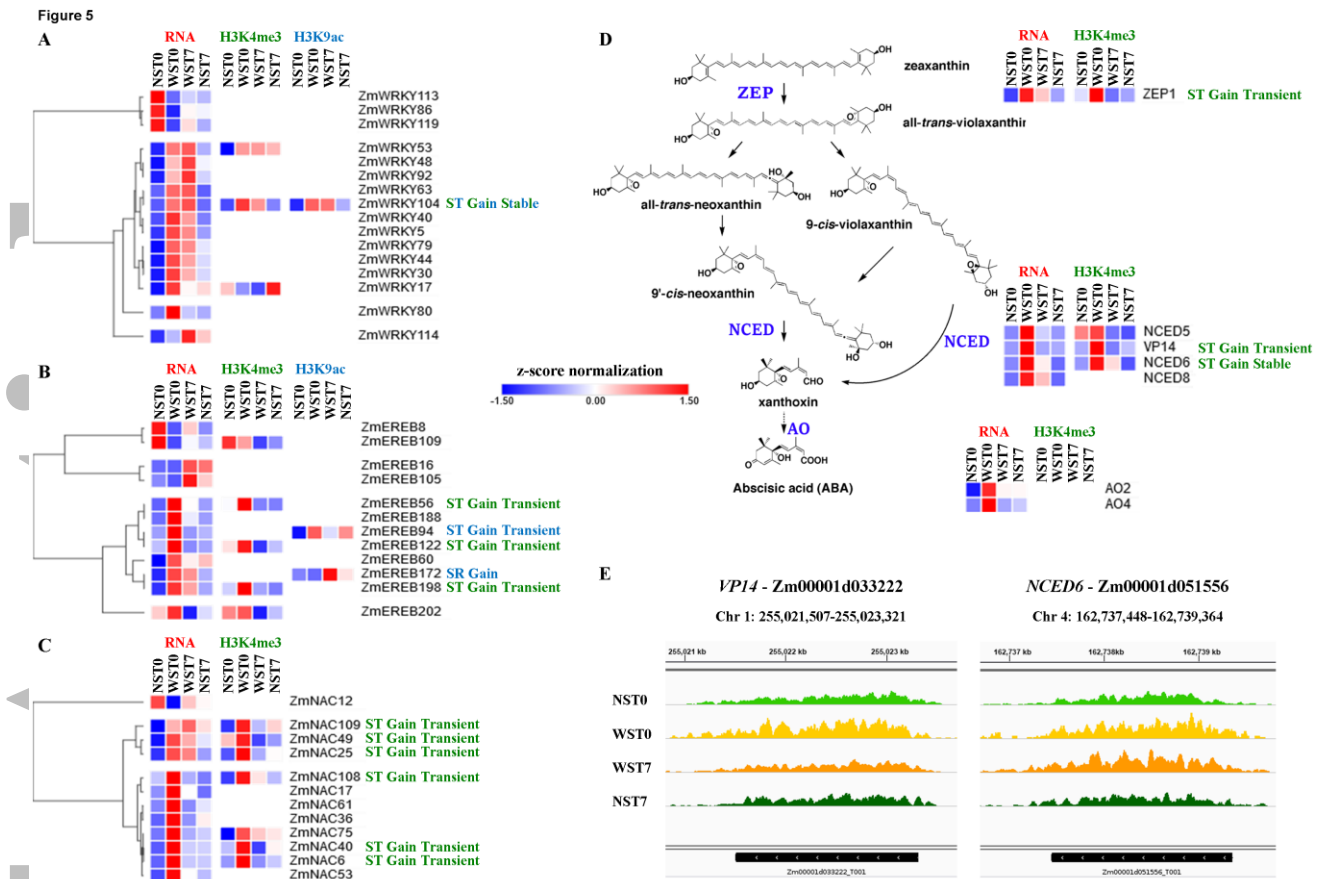


Figure 5. Transcriptomic and epigenomic status of genes associated to drought stress response.

Integrative analysis of RNA-Seq and Chip-Seq data for WRKY (A), EREBP (B) NAC (C) transcription factor coding genes and abscisic acid (ABA) biosynthetic enzymes (D and E) coding genes differentially expressed in response to drought and recovery. Heat maps (A-D) show, for the four samples, the z-score scaled gene expression levels (RPKM) and, for DEGs being also DMGs, the scaled ChIP-Seq read counts. The signatures of the chromatin profile cluster the genes belong to are color-coded accordingly to the specific histone mark: light green for H3K4me3 and light blue for H3K9ac. Heat maps for ABA biosynthesis coding genes (D) are placed close to a schematic representation of the hormone biosynthesis pathway. ChIP-Seq normalized H3K4me3 tracks (E) show the different enrichment dynamics at *VPI4* and *NCED6* loci. ZEP: zeaxanthin epoxidase; NCED: 9-cis-epoxycarotenoid dioxygenase; AO: aldehyde oxidase.

Accepted Article

Figure 6

A



B

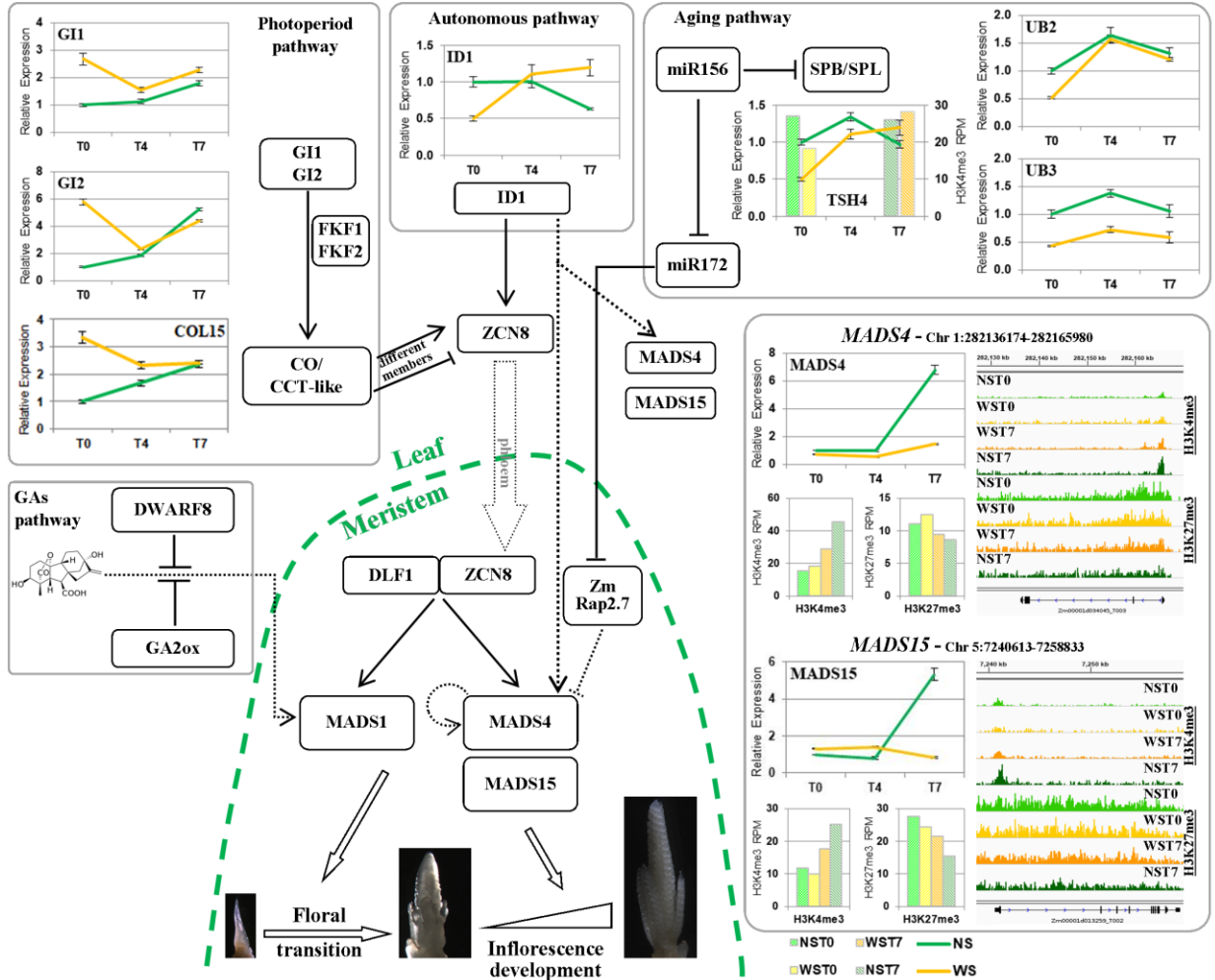


Figure 6. Transcriptomic and epigenomic status of genes associated to flowering transition and inflorescence patterning.

(A) Integrative analysis of RNA-Seq and Chip-Seq data for candidate floral regulators coding genes differentially expressed in response to drought and recovery. Heat maps show, for the four samples, the z-score scaled gene expression levels (RPKM) and, for DEGs being also DMGs, the scaled ChIP-Seq read counts. The signature of the chromatin profile cluster the genes belong to are color-coded accordingly to the specific histone mark: light green for H3K4me3, light blue for H3K9ac and violet for H3K27me3. (B) Schematic representation of maize flowering time controlling pathways acting in the leaf, the shoot apical meristem (SAM) or potentially both. Known relationships between genes are shown with arrows or T lines, designating positive (activation) and negative (suppression) regulation, respectively. Signals from the photoperiod and autonomous pathway are physically transduced from leaves to the SAM by ZCN8 protein via movement through the phloem. Dashed lines stand for putative relationship derived through comparative genomics. The expression dynamics of nine DEGs has been investigated also at an intermediate time-point during the recovery period (NST4 and WST4) by qRT-PCR, and the results are reported in the inset line graphs, while bar charts summarize normalized ChIP-Seq mapped reads at *TASSEL SHEAT4* (*TSH4*), *MADS4* and *MADS15* loci. ChIP-Seq normalized H3K4me3 and H3K27me3 tracks clearly show the different enrichment dynamics at *MADS4* and *MADS15* loci.

Figure 7

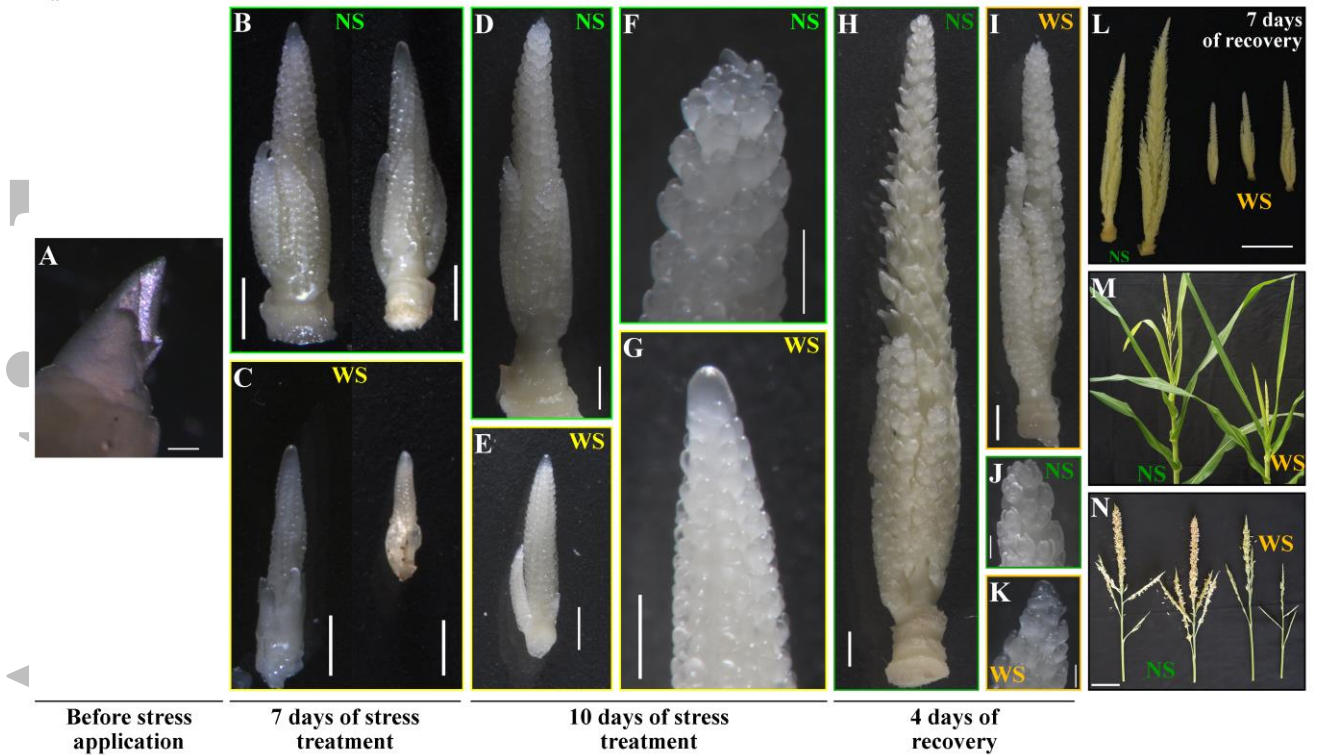


Figure 7. Delayed and altered male inflorescence development during the course of the stress plus recovery experiment and at maturity.

Representative images of shoot apices (A) immature tassels (B-L) and mature male inflorescences (M-N) dissected just before the drought stress application (A), during the ten days of progressive dehydration stress (B-G) and during the recovery stage (H-L).

Inflorescences isolated from stressed plants (WS) are shorter and with fewer and smaller branch primordia compared to control ones (NS), during the whole course of the drought plus recovery experiment (B-E, H-I, and L). Drought stress-induced developmental delay results in the retain of floral meristem indeterminacy at the end of the stress application (F-G) and also after 4 days of recovery (J-K) and the alterations in tassel size persist until tasseling and anthesis stages (M-N). Two inflorescences dissected from independent stressed and control plants are reported in panels B and C. Scale bars = 500 μ m in A to K, 1 cm in L and 5 cm in N.